

ADAPTIVE ROLLOUT ALLOCATION FOR ONLINE REINFORCEMENT LEARNING WITH VERIFIABLE REWARDS

006 **Anonymous authors**

007 Paper under double-blind review

ABSTRACT

013 Sampling efficiency is a key bottleneck in reinforcement learning with verifiable
 014 rewards. Existing group-based policy optimization methods, such as GRPO, allo-
 015 cate a fixed number of rollouts for all training prompts. This uniform allocation
 016 implicitly treats all prompts as equally informative, and could lead to inefficient
 017 computational budget usage and impede training progress. We introduce VIP,
 018 a Variance-Informed Predictive allocation strategy that allocates a given rollout
 019 budget to the prompts in the incumbent batch to minimize the expected gradient
 020 variance of the policy update. At each iteration, VIP uses a lightweight Gaussian
 021 process model to predict per-prompt success probabilities based on recent roll-
 022 outs. These probability predictions are translated into variance estimates, which
 023 are then fed into a convex optimization problem to determine the optimal rollout
 024 allocations under a hard compute budget constraint. Empirical results show that
 025 VIP consistently improves sampling efficiency and achieves higher performance
 026 than uniform or heuristic allocation strategies in multiple benchmarks.

1 INTRODUCTION

029 The advent of Language Models (LMs) has marked a new era in artificial intelligence, transforming
 030 models from static knowledge bases into dynamic, intelligent agents capable of complex reasoning,
 031 creative generation, and intricate problem-solving. This evolution has been largely driven by the ad-
 032 vancement of post-training methodologies, which are crucial for aligning a base LM’s vast, general
 033 knowledge with specific human intentions, ethical guidelines, and desired task-oriented behaviors.
 034 These refinement processes bridge the gap between a model that understands language and one that
 035 can reliably and safely act as a collaborator, assistant, or autonomous agent. As LMs become more
 036 integrated into real-world applications, the effectiveness and efficiency of these post-training stages
 037 have become a primary focus of research and development.

038 Two prominent paradigms are used for post-training LMs: Supervised Fine-Tuning (SFT) and Re-
 039 enforcement Learning (RL). SFT is a computationally efficient approach that trains the model on a
 040 curated dataset of input-output pairs, effectively equipping it with domain-specific knowledge. How-
 041 ever, its effectiveness is often hampered by the difficulty of curating high-quality and comprehensive
 042 datasets. In contrast, RL-based methods, which treat the model as an agent optimizing for a reward
 043 signal derived from human preferences (Reinforcement Learning from Human Feedback, RLHF)
 044 or external verification mechanisms (Reinforcement Learning from Verifiable Rewards, RLVR), can
 045 explore a broader action space and achieve superior performance on complex, open-ended tasks.
 046 RLVR, in particular, has gained wide popularity thanks to its low reliance on human input. How-
 047 ever, the performance of RL methods comes at a significant computational cost. Algorithms like
 048 Proximal Policy Optimization (PPO, Schulman et al. (2015)) require the simultaneous training of
 049 a separate value model to estimate the advantage of actions, which can be prohibitively memory-
 050 intensive in resource-constrained situations. To address this, a family of “critic-free” or group-based
 051 RL methods has emerged, estimating the advantage as a relative measure within a group of roll-
 052 outs, essentially trading speed for memory efficiency. Such methods include GRPO, (Shao et al.,
 053 2024), Dr. GRPO (Liu et al., 2025), RLOO (Ahmadian et al., 2024), and other variants. A direct
 054 drawback of these methods is the additional computation time required to generate multiple roll-
 055 outs for a training example. The number of generations often needs to be large enough (e.g., 16)

054 to obtain a stable training process, which exacerbates the generation overhead and eventually leads
 055 to a memory-bound system. Such high computational demands consequently highlight the need for
 056 greater sampling efficiency in the RL training process.

057 The high computational demands of RL algorithms have led to a body of work dedicated to optimizing
 058 this performance-cost trade-off. One line of research involves hybrid approaches that combine an
 059 initial SFT phase with a subsequent RL refinement stage (Chen et al., 2025a) or merge the two stages
 060 into a single method (Fu et al., 2025). These methods demonstrated improvement in smoothening
 061 or even accelerating the training process, but often fail to dynamically adapt to the training process
 062 based on the model’s evolving capabilities for solving the training problems. The observation that
 063 simply filtering out problems where the accuracy is close to either 0 or 1 can boost performance (Yu
 064 et al., 2025) hints at the potential for more adaptive control. To the best of our knowledge, there
 065 is a lack of crucial metrics for such capabilities and, consequently, a lack of an adaptive control
 066 mechanism for the GRPO process.

067 To address such challenges, we introduce the Variance-Informed Predictive allocation strategy
 068 (VIP), a principled training framework for efficient and adaptive rollout allocation in group-based
 069 policy optimization. We first provide a theoretical analysis of the gradient variance for three prominent
 070 RL algorithms, establishing the relationship between the gradient variance contributed by a
 071 prompt and the probability that it is solved by the current model. Building on this insight, at the
 072 beginning of each training iteration, VIP predicts the expected gradient variance of each prompt in
 073 a mini-batch. Based on these predictions, VIP then solves a convex optimization problem followed
 074 by integer rounding heuristic to allocate rollouts across prompts to minimize the total expected
 075 gradient variance under the given computational budget. The core contributions of this paper are the
 076 following:

- 077 • **Gradient variance analysis.** We provide a rigorous analysis of the effect of gradient variance on
 078 the RL training process. We derive the connection between gradient variance and success probability
 079 for prevailing group-based RL methods, including Dr. GRPO and RLOO. This establishes
 080 the theoretical foundation for adaptively controlling budget allocation during training.
- 081 • **Variance prediction.** VIP employs a Gaussian process (GP) over prompt embeddings to model
 082 the probability of success for each prompt in any training step. This enables recursive Bayesian
 083 updates that leverage both past rollout outcomes and the similarity structure of the prompts. The
 084 GP prediction allows the framework to estimate the gradient variance for each prompt in the
 085 minibatch at every training step.
- 086 • **Variance-minimizing rollout allocation.** Given the predicted variances, VIP formulates a convex
 087 optimization problem to determine the optimal allocation of rollouts on prompts. This allocation
 088 minimizes the gradient variance subject to a rollout budget constraint. We derive an
 089 efficient algorithm that provides the exact solution to the continuous relaxation and further develop
 090 a greedy incentive-based rounding heuristic to produce a feasible integer solution. This
 091 process enables fast resource allocation under computational budget constraints.

092 Our paper unfolds as follows. Section 2 discusses related work on adaptive strategies over group-based
 093 RL frameworks for RLVR, while Section 3 lays the technical background on RLVR. Section 4
 094 presents our analysis of the per-prompt gradient variance. Section 5 delineates our VIP framework
 095 for variance prediction via Gaussian process, and the optimization problem for rollout allocation.
 096 Section 6 presents empirical results on mathematical reasoning and information retrieval datasets.

100 2 RELATED WORK

101 Recent advancements in group-based RL for LMs have focused on adaptive strategies to enhance
 102 both training efficiency and performance. These methods move beyond static training pipelines
 103 by dynamically selecting and managing data used for policy updates. Initial research empirically
 104 demonstrated that filtering out “non-informative” problems to which the model’s accuracy is either
 105 0 or 1 can improve training efficiency, as these problems lead to rollout batches with zero variance
 106 and consequently make no contribution to the gradient signal (Yu et al., 2025). Along similar lines,
 107 (Lin et al., 2025) filtered out rollouts with low absolute advantage, while (Xu et al., 2025) proposed
 to retain examples with the highest variance. Lacking an a priori measure of training prompt infor-

108 mativity, these methods require the pre-sampling of a large batch of rollouts before each update
 109 iteration, potentially negating efficiency gains from the significant sampling overhead.
 110

111 Several works adopted a pre-rollout estimation of the prompt informativeness. (Zheng et al., 2025)
 112 proposed skipping each problem with a probability determined by the number of recent consecutive
 113 rollouts where the prompt is non-informative. (Zhang et al., 2025) proposed a signal-to-noise ratio
 114 indicating a problem’s contribution to the gradient, and showed that training can be accelerated by
 115 generating a small trial batch of rollouts to identify and filter out non-informative problems, and then
 116 continue sampling on intermediate-difficulty ones. (Sun et al., 2025) designed a difficulty-targeted
 117 online selection algorithm with attention-based difficulty prediction and rollout replay. (Liao et al.,
 118 2025) ranked problems by difficulty, indicated by the average rewards from past rollouts, and al-
 119 located resources to sample larger batches for difficult prompts. (Yang et al., 2025) took a similar
 120 approach as (Zhang et al., 2025) to estimate problem difficulty, and assigned a larger budget and
 121 higher gradient weights to difficult prompts. (Kong et al., 2025) estimates prompt difficulty by ag-
 122 gregating historical performance discrepancies of the problems, then adaptively selects the set of
 123 problems whose difficulty is in alignment with the current competence of the model. Other works
 124 also considered the entropy-reward trade-off to mitigate the risk of premature convergence. (Liao
 125 et al., 2025) combined difficulty-aware reallocation with entropy-stabilizing temperature scheduling
 126 to effectively balance efficiency and exploration. Another approach steers exploration by maximiz-
 127 ing information gain throughout the training process (Lee et al., 2024).
 128

3 BACKGROUND ON RLVR

130 We study the prominent family of methods for RL training that employs group-based advantage
 131 estimation to stabilize learning and better utilize reward signals. This family includes Group Relative
 132 Policy Optimization (GRPO)(Shao et al., 2024) and its variants, such as Dr. GRPO (Liu et al., 2025)
 133 and RLOO (Ahmadian et al., 2024). Given a dataset of Q prompts $\mathcal{Q} = \{q_1, q_2, \dots, q_Q\}$, the general
 134 objective function for group-based policy optimization methods is

$$135 \quad J(\theta) = \mathbb{E}_{q \sim \mathcal{Q}} \mathbb{E}_{\pi_{\text{old}}^{\otimes n}} \left[\frac{1}{n} \sum_{j=1}^n \frac{1}{|\tilde{o}_j|} \sum_{\tau=1}^{|\tilde{o}_j|} \left(A'_{j,\tau} - \beta D_{\text{KL}}(\pi_{\theta}(\cdot | q, \tilde{o}_{j,<\tau}) \| \pi_{\text{ref}}(\cdot | q, \tilde{o}_{j,<\tau})) \right) \right], \quad (1)$$

139 where n is the number of rollouts for each prompt, \tilde{o}_j is the j -th rollout from policy π_{old} , $|\tilde{o}_j|$ is
 140 the number of tokens in \tilde{o}_j , and π_{θ} is the current policy with its learnable parameters θ . Here,
 141 $D_{\text{KL}}(\pi_{\theta}(\cdot | q, \tilde{o}_{j,<\tau}) \| \pi_{\text{ref}}(\cdot | q, \tilde{o}_{j,<\tau}))$ is the Kullback-Leibler divergence between the policy π_{θ}
 142 and a reference policy π_{ref} , both of which are conditioned on the prompt q and the tokens generated
 143 thus far $\tilde{o}_{j,<\tau}$. We use a tilde (\sim) to emphasize the stochastic nature of the quantities.

144 For prompt q , the term $A'_{j,\tau}$ is the normalized or advantage-shaped reward at token τ for output \tilde{o}_j :
 145

$$146 \quad A'_{j,\tau} = \min \left(r_{j,\tau} \tilde{A}_{j,\tau}, \text{clip}(r_{j,\tau}, 1 - \epsilon, 1 + \epsilon) \tilde{A}_{j,\tau} \right), \quad \text{with} \quad r_{j,\tau}(\theta) = \frac{\pi_{\theta}(\tilde{o}_{j,\tau} | q, \tilde{o}_{j,<\tau})}{\pi_{\text{old}}(\tilde{o}_{j,\tau} | q, \tilde{o}_{j,<\tau})}. \quad (2)$$

148 Notice that we momentarily omit the index q to avoid clutter. Here, $r_{j,\tau}$ is the relative ratio between
 149 current and data-generating policies; while $\tilde{A}_{j,\tau}$ is the advantage estimator for token τ in output \tilde{o}_j .
 150 Let $R(\tilde{o}_j)$ be the reward for output \tilde{o}_j on prompt q , taking values of -1 (incorrect) or 1 (correct).
 151 Based on the whole set of n rollouts $\{\tilde{o}_j\}$, there are two popular advantage estimators:
 152

- 153 • In Dr. GRPO (Liu et al., 2025), $\tilde{A}_j = \tilde{A}_{j,\tau} = R(\tilde{o}_j) - \frac{1}{n} \sum_k R(\tilde{o}_k)$, which uses all rollouts to
 154 compute the mean.
- 155 • In RLOO (Ahmadian et al., 2024), $\tilde{A}_j = \tilde{A}_{j,\tau} = R(\tilde{o}_j) - \frac{1}{n-1} \sum_{k \neq j} R(\tilde{o}_k)$, which excludes the
 156 j -th output when computing the mean.

158 Both advantage estimators are token-independent: all tokens in the j -th rollout admit the same
 159 advantage \tilde{A}_j . In this paper, we will focus on a particular training regime under the next assumption.
 160

161 **Assumption 3.1.** *We set the KL regularization term to zero, i.e., $\beta = 0$.*

162 Assumption 3.1 is both practical and non-restrictive for the following reasons. In RLHF, reward
 163 models are only reliable near the distribution of the reference policy (Gao et al., 2023; Chen et al.,
 164 2024; Huang et al., 2024; Ramé et al., 2024), which makes KL regularization essential to prevent
 165 reward hacking (Laidlaw et al., 2024; Song et al., 2024; Skalse et al., 2022). In contrast, our work
 166 focuses on the RLVR setting, where rewards are computed by rule-based verifiers. These verifiable
 167 rewards eliminate concerns about reward miscalibration. Indeed, recent studies in RLVR have suc-
 168 cessfully removed the KL term while still achieving state-of-the-art performance (Yu et al., 2025;
 169 Liu et al., 2025).

170 Assumption 3.1 simplifies the training objective by eliminating the KL term. The objective function
 171 reduces to:

$$173 J(\theta) = \mathbb{E}_{q \in \mathcal{Q}} \mathbb{E}_{\pi_{\text{old}}^{\otimes n}} \left[\frac{1}{n} \sum_{j=1}^n \frac{1}{|\tilde{o}_j|} \sum_{\tau=1}^{|\tilde{o}_j|} \min \left(r_{j,\tau} \tilde{A}_j, \text{clip}(r_{j,\tau}, 1-\epsilon, 1+\epsilon) \tilde{A}_j \right) \right]$$

175 Whenever $r_{j,\tau}$ falls outside the clipping region in a direction that worsens the surrogate,
 176 $\min \left(r_{j,\tau} \tilde{A}_j, \text{clip}(r_{j,\tau}, 1-\epsilon, 1+\epsilon) \tilde{A}_j \right)$ collapses to the clipped term and contributes no gradient.
 177 To isolate precisely when the gradient is active, we introduce the indicator

$$180 \mathbb{I}_{j,\tau}^{\text{unc}} = 1 - \left(\mathbf{1}\{r_{j,\tau} > 1+\epsilon\} \mathbf{1}\{\tilde{A}_j \geq 0\} + \mathbf{1}\{r_{j,\tau} < 1-\epsilon\} \mathbf{1}\{\tilde{A}_j < 0\} \right).$$

182 Using this indicator, we define $\bar{r}_j = \frac{1}{|\tilde{o}_j|} \sum_{\tau=1}^{|\tilde{o}_j|} \mathbb{I}_{j,\tau}^{\text{unc}} r_{j,\tau}$ and rewrite the objective as:

$$184 J(\theta) = \mathbb{E}_{q \in \mathcal{Q}} \mathbb{E}_{\pi_{\text{old}}^{\otimes n}} \left[\frac{1}{n} \sum_{j=1}^n \tilde{A}_j \bar{r}_j \right] = \mathbb{E}_{q \in \mathcal{Q}} \mathbb{E}_{\pi_{\text{old}}^{\otimes n}} \left[\frac{1}{n} \sum_{j=1}^n A_j(\{\tilde{o}_k\}) \bar{r}_j \right]. \quad (3)$$

187 The next section studies the gradient variance of J .

190 4 ANALYSIS FOR GRADIENT VARIANCE

192 In this section, we analyze the variance of the gradient estimator arising from sampling rollouts in
 193 RLVR algorithms such as GRPO and RLOO. Each update step combines two types of data: previ-
 194 ously collected rollouts from past batches (off-policy) and newly generated rollouts for the current
 195 batch of prompts \mathcal{B} (on-policy). However, as discussed in the subsequent Section 5, our research
 196 objective is to determine how many rollouts should be allocated to the prompts in \mathcal{B} . This alloca-
 197 tion decision influences only the on-policy component of the gradient. The off-policy contributions,
 198 while present in the overall update, are determined entirely by past data and therefore remain un-
 199 affected by the number of new rollouts we choose to sample. Consequently, to understand how
 200 allocation impacts gradient variance, it is both natural and sufficient to isolate the variance arising
 201 from the on-policy rollouts generated by the current policy π_θ . For these on-policy samples, the
 202 behavior and target policies coincide $\pi_{\text{old}} = \pi_\theta$, hence $\bar{r}_j = 1$.

203 The gradient contribution of these on-policy rollouts is:

$$204 \nabla_\theta J^{\text{on}}(\theta) = \mathbb{E}_{q \in \mathcal{B}} \mathbb{E}_{\pi_\theta^{\otimes n}} \left[\frac{1}{n} \sum_{j=1}^n A_j(\{\tilde{o}_k\}) \underbrace{\frac{1}{|\tilde{o}_j|} \sum_{\tau=1}^{|\tilde{o}_j|} \nabla_\theta \log \pi_\theta(\tilde{o}_{j,\tau} | q, \tilde{o}_{j,<\tau})}_{\triangleq H(\tilde{o}_j)} \right]. \quad (4)$$

209 Above, $H(\tilde{o}_j)$ is the average log-likelihood gradient, where the average is taken over all tokens
 210 in the j -th rollout. Consider a specific prompt q and the n rollouts $\{\tilde{o}_k\}$, the contribution of q to
 211 the calculation of the sample gradient is $\frac{1}{n} \sum_{j=1}^n A_j(\{\tilde{o}_k\}) H(\tilde{o}_j)$, and we omit the subscript q to
 212 avoid clutter. This quantity is a random vector because $H(\tilde{o}_j)$ is a random vector. We will study the
 213 *projected* gradient, obtained by projecting $H(\tilde{o}_j)$ onto the vector $\mathbb{1}$ of all ones. To this end, we are
 214 interested in the (univariate) random variable:

$$215 \tilde{G} \triangleq \frac{1}{n} \sum_{j=1}^n A_j(\{\tilde{o}_k\}) \mathbb{1}^\top H(\tilde{o}_j).$$

To simplify the notation, we define the random variables $\tilde{R}_j = R(\tilde{o}_j)$ and $\tilde{Z}_j = \mathbb{1}^\top H(\tilde{o}_j)$ for all j . We first consider the Dr. GRPO case. The gradient \tilde{G} has the specific form:

$$\tilde{G} \triangleq \frac{1}{n} \sum_{j=1}^n (\tilde{R}_j - \frac{1}{n} \sum_{k=1}^n \tilde{R}_k) \tilde{Z}_j.$$

To have a rigorous analysis of the variance of \tilde{G} , we make the following assumption explicitly.

Assumption 4.1. (i) $\tilde{R}_1, \dots, \tilde{R}_n$ are independent and identically distributed (i.i.d.) copies of \tilde{R} , and $\tilde{Z}_1, \dots, \tilde{Z}_n$ are also i.i.d. copies of \tilde{Z} ,

(ii) $\{\tilde{Z}_j\}$ and $\{\tilde{R}_j\}$ are uncorrelated up to second-order: $\text{Cov}(\tilde{R}_k, \tilde{Z}_j) = 0$ for any (k, j) and $\text{Cov}(\tilde{R}_k \tilde{R}_{k'}, \tilde{Z}_j \tilde{Z}_{j'}) = 0$ for any (k, j, k', j')

Assumption 4.1 is realistic in common settings: given the same prompt and fixed sampling procedure, different rollouts are independent samples from the same distribution π_θ . Thus, it is reasonable to assume that $\{\tilde{o}_j\}$ are i.i.d., which induces Assumption 4.1(i). Assumption 4.1(ii) needs further justification because for the j -th rollout, the reward \tilde{R}_j may be correlated with the average gradient \tilde{Z}_j . However, we have strong reasons to believe that it holds because \tilde{R} is a Bernoulli distribution, and \tilde{Z}_j has a doubly-averaging nature over the number of tokens (from the definition of $H(\tilde{o}_j)$) and over the number of dimensions in the gradient vector (from $\mathbb{1}^\top H(\tilde{o}_j)$). Empirically, we include in Appendix B a statistical test to support our assumption.

The next result establishes the variance for the Dr. GRPO case.

Proposition 4.2 (Dr. GRPO gradient variance). *Consider a prompt with binary reward $R(\tilde{o}_j) \in \{1, -1\}$ with $\mathbb{P}(R(\tilde{o}_j) = 1) = p$. If Assumption 4.1 holds and the variance of the projected gradient \tilde{Z} is σ_Z^2 , the variance of the per-prompt projected Dr. GRPO gradient estimator with n rollouts is*

$$\text{Var}(\tilde{G}) = \frac{(n-1)}{n^2} 4\sigma_Z^2 p(1-p).$$

We now switch gears to the RLOO case. The RLOO gradient \tilde{G} has the specific form:

$$\tilde{G} \triangleq \frac{1}{n} \sum_{j=1}^n (\tilde{R}_j - \frac{1}{n-1} \sum_{k \neq j}^n \tilde{R}_k) \tilde{Z}_j.$$

Proposition 4.3 (RLOO gradient variance). *Consider a prompt with binary reward $R(\tilde{o}_j) \in \{1, -1\}$ with $\mathbb{P}(R(\tilde{o}_j) = 1) = p$. If Assumption 4.1 holds and the variance of the projected gradient \tilde{Z} is σ_Z^2 , the variance of the per-prompt projected RLOO gradient estimator with n rollouts is*

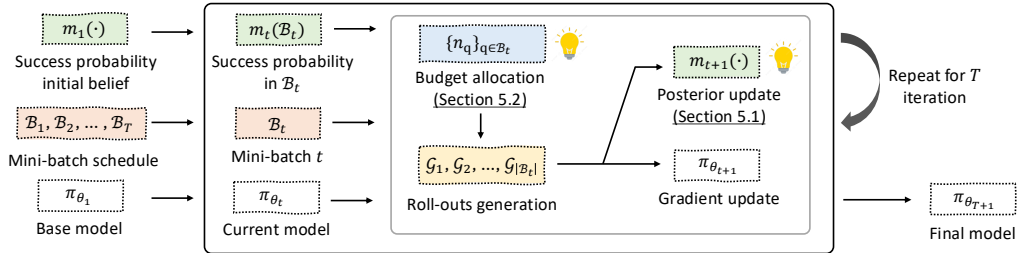
$$\text{Var}(\tilde{G}) = \frac{1}{n-1} 4\sigma_Z^2 p(1-p).$$

5 PREDICTIVE ROLLOUT ALLOCATION STRATEGY

Consider a specific iteration t when we have drawn a mini-batch \mathcal{B}_t from the set of training prompts. Propositions 4.2-4.3 indicate that the gradient variance for a prompt depends on the number of rollouts. Consequently, a uniform allocation of n rollouts for every prompt could be inefficient. Section 4 reveals that the per-prompt gradient variance depends on the success probability p_q , which is the probability that model θ_t answers prompt q correctly. However, this probability is not observable ex ante without performing rollouts, and we need to resort to an estimate \hat{p}_q to make allocation decisions. Building an estimator for the success probability is challenging for at least two reasons: First, the success probability is, unfortunately, not static: it depends on the model weights, which evolve after every training iteration. As the weights are updated, the distribution over the outputs changes, and consequently, the success probability drifts. Second, prompt embeddings may not contain sufficiently informative signal for parametric classifiers.

To improve rollout efficiency, we propose VIP, the Variance-Informed Predictive allocation strategy, which minimizes the minibatch gradient variance by allocating a different number of rollouts $\{n_q\}$ for each prompt in the minibatch. The complete workflow of VIP, from prediction to optimized rollout allocation, is illustrated in Figure 1. VIP comprises two main components: (i) a nonparametric

270 Gaussian process model for predicting the success probability of the current model on each training
 271 prompt (green boxes), and (ii) an optimization model for making optimal allocation decisions given
 272 the computing budget (blue box). At the beginning of iteration t , we first predict the success prob-
 273 ability for all $q \in \mathcal{B}_t$, as described in Section 5.1. The probability estimates serve as input to our
 274 optimization framework for allocating rollouts across prompts in Section 5.2.
 275



285 Figure 1: The process starts with an initial belief over prompt success probabilities. At each step
 286 t , a mini-batch \mathcal{B}_t is selected, and the belief function $m_t(\cdot)$ predicts the success probabilities of the
 287 prompts in \mathcal{B}_t . A budget allocation module assigns rollout budgets $\{n_q\}$, rollouts are generated, and
 288 the resulting data updates the model and beliefs. Repeated for T steps, this yields a fine-tuned model
 289 $\pi_{\theta_{T+1}}$ with improved performance and efficient rollout usage.

5.1 GP PRIOR AND RECURSIVE POSTERIOR UPDATE

290 Given the training prompts $\mathcal{Q} = \{q_1, q_2, \dots, q_Q\}$, we denote their embeddings as $\mathcal{D} = \{x_q\}_{q=1}^Q$.
 291 At every iteration t , the success probability of the current model on prompt q is modeled using a
 292 sigmoid link function on the latent value $g_t(x_q)$:

$$293 p_{q,t} = \text{sigmoid}(g_t(x_q)) = 1/[1 + \exp(-g_t(x_q))] \in (0, 1),$$

294 where $g_t : \mathbb{R}^d \rightarrow \mathbb{R}$ is a latent function over prompt embeddings. Because g_t is real-valued, it
 295 is simpler to place a Gaussian process on g_t . Toward this goal, we set $g_t \sim \text{GP}(m_t(\cdot), \mathcal{K}(\cdot, \cdot))$,
 296 where m_t is the mean function and \mathcal{K} is a radial basis function (RBF) kernel with bandwidth $h > 0$:

$$297 \mathcal{K}(x, x') = \exp(-\|x - x'\|_2^2/(2h^2)).$$

300 **Initialization.** At $t = 1$, we use a zero-mean prior $g_1 \sim \text{GP}(0, \mathcal{K})$. Over the dataset $\mathcal{D} = \{x_q\}_{q=1}^Q$,
 301 this gives $g_1(\mathcal{D}) \sim \mathcal{N}(0, \Sigma)$ where $\Sigma = \mathcal{K}(\mathcal{D}, \mathcal{D})$ is the kernel matrix over all prompts.

303 **Prediction.** At iteration t , the prior m_t is used to predict $\hat{p}_{q,t} = \text{sigmoid}(m_t(x_q))$ for $q \in \mathcal{B}_t$. These
 304 predicted values will be sent to the optimization problem to compute the rollout allocation.

305 **Sequential updates.** At iteration $t \geq 1$, the latent values for all prompts are captured by a random
 306 vector $[g_t(x_1), \dots, g_t(x_Q)]^\top \sim \mathcal{N}(m_t, \Sigma)$. For $q \in \mathcal{B}_t$, we observe n_q rollouts and rewards $\tilde{R}_{q,j} \in$
 307 $\{-1, 1\}$ for $j = 1, \dots, n_q$. Then, we compute the clipped average:

$$308 \tilde{R}_q = \frac{1}{n_q} \sum_{j=1}^{n_q} \tilde{R}_{q,j} \in [-1, 1], \quad \hat{p}_{q,t} = \text{clip}\left(\frac{\tilde{R}_q + 1}{2}, \epsilon, 1 - \epsilon\right) \in (\epsilon, 1 - \epsilon),$$

311 which induces an observation for the latent value $\hat{g}_{q,t} = \text{sigmoid}^{-1}(\hat{p}_{q,t}) \in \mathbb{R}$ for $q \in \mathcal{B}_t$. Clipping
 312 is necessary here to avoid the situation when $\tilde{R}_{q,t} = -1$ or 1 , which leads to infinite values for the
 313 latent variable. The collection of these latent values is denoted $\hat{g}_{\mathcal{B}_t}$. Let \mathcal{B}_t^c be the complement set
 314 containing all prompts that are *not* in the mini-batch \mathcal{B}_t . We can partition the mean vector and the
 315 covariance matrix into the block form:

$$316 m_t = \begin{bmatrix} m_{t,\mathcal{B}_t} \\ m_{t,\mathcal{B}_t^c} \end{bmatrix}, \quad \Sigma = \begin{bmatrix} \Sigma_{\mathcal{B}_t \mathcal{B}_t} & \Sigma_{\mathcal{B}_t \mathcal{B}_t^c} \\ \Sigma_{\mathcal{B}_t^c \mathcal{B}_t} & \Sigma_{\mathcal{B}_t^c \mathcal{B}_t^c} \end{bmatrix},$$

318 the posterior over unqueried prompts at iteration t is $g_{t,\mathcal{B}_t^c} \mid \hat{g}_{\mathcal{B}_t} \sim \mathcal{N}(m_t^*, \Sigma^*)$ with

$$320 m_{t,\mathcal{B}_t^c}^* = m_{t,\mathcal{B}_t^c} + \Sigma_{\mathcal{B}_t^c \mathcal{B}_t} \Sigma_{\mathcal{B}_t \mathcal{B}_t}^{-1} (\hat{g}_{\mathcal{B}_t} - m_{t,\mathcal{B}_t}), \quad \Sigma^* = \Sigma_{\mathcal{B}_t^c \mathcal{B}_t^c} - \Sigma_{\mathcal{B}_t^c \mathcal{B}_t} \Sigma_{\mathcal{B}_t \mathcal{B}_t}^{-1} \Sigma_{\mathcal{B}_t \mathcal{B}_t^c}.$$

322 **Next-step prior.** The prior mean at iterate t is updated into the posterior mean as follows: we set
 323 $m_{t+1}(x_q) = \hat{g}_{q,t}$ if $q \in \mathcal{B}_t$ and set $m_{t+1}(x_q) = m_{t,\mathcal{B}_t^c}^*(x_q)$ if $q \in \mathcal{B}_t^c$. This posterior mean m_{t+1}
 324 will serve as the prior in iteration $t + 1$.

324
325

5.2 ADAPTIVE BUDGET ALLOCATION FOR GRADIENT VARIANCE MINIMIZATION

326
327
328
329
330
331
332

Consider a mini-batch \mathcal{B}_t of B prompts, and every prompt $q \in \mathcal{B}_t$ has a *predicted* success probability \hat{p}_q under the GP model from Section 5.1. We now focus on deciding the number of rollouts $\{n_q\}$ assigned to each prompt in this batch \mathcal{B}_t under a hard constraint of a total budget of C rollouts. Additionally, we impose that the number of rollouts should be between a lower bound L and an upper bound U : if the number of rollouts is too small, it is unlikely to obtain discriminative reward signals, while a large number of rollouts may lead to overfitting. For a meaningful setting, we require $L \geq 3$, and assume that $BL \leq C \leq BU$.

333
334

Our objective is to minimize the sum of the gradient variance induced by prompts in the mini-batch \mathcal{B}_t . This problem can be formulated as an integer optimization problem:

335
336
337

$$\min \left\{ \sum_{q \in \mathcal{B}_t} \text{Var}(\tilde{G}_q) : \sum_{q \in \mathcal{B}_t} n_q = C, \quad n_q \in \{L, L+1, \dots, U\} \quad \forall q \in \mathcal{B}_t \right\}. \quad (5)$$

338
339
340

The variance $\text{Var}(\tilde{G}_q)$ is likely a nonlinear function of the rollout allocation n_q , and (5) becomes a nonlinear integer optimization problem. To tackle this problem, we will first solve its continuous relaxation and then apply a heuristic rounding algorithm.

341
342
343

Relaxed Solution for Budget Allocation. Proposition 4.2 provides the per-prompt gradient variance $\text{Var}(\tilde{G}_q)$ for Dr. GRPO. By defining $a_q \triangleq 4\sigma_{Z_q}^2 \hat{p}_q(1 - \hat{p}_q)$ for every $q \in \mathcal{B}_t$, the continuous relaxation of problem (5) for Dr. GRPO is

344
345
346

$$\min \left\{ \sum_{q \in \mathcal{B}_t} a_q \frac{n_q - 1}{n_q^2} : \sum_{q \in \mathcal{B}_t} n_q = C, \quad L \leq n_q \leq U, \quad n_q \in \mathbb{R} \forall q \in \mathcal{B}_t \right\}. \quad (6)$$

347

The next theorem asserts a computationally efficient method to solve (6).

348
349

Theorem 5.1 (Continuous allocation, Dr. GRPO). *For each $q \in \mathcal{B}_t$, let n_q^* be the function:*

350
351
352
353
354

$$n_q^*(\lambda) = \begin{cases} U & \text{if } \lambda \leq a_q \frac{U-2}{U^3}, \\ \text{the unique solution to } \lambda = a_q \frac{n_q-2}{n_q^3} & \text{if } a_q \frac{U-2}{U^3} < \lambda < a_q \frac{L-2}{L^3}, \\ L & \text{if } \lambda \geq a_q \frac{L-2}{L^3}. \end{cases} \quad (7)$$

355
356
357

If $BL \leq C \leq BU$, the algebraic equation $\sum_q n_q^*(\lambda^*) = C$ has a unique solution λ^* . Then the unique minimizer of (6) is given by $n_q^* = n_q^*(\lambda^*)$ for all q . Moreover, λ^* can be found by bisection.

358
359
360

Similarly, for the RLOO case, we can leverage Proposition 4.3 to define the same parameters $a_q \triangleq 4\sigma_{Z_q}^2 \hat{p}_q(1 - \hat{p}_q)$ for $q \in \mathcal{B}_t$. The continuous relaxation of (5) for RLOO is

361
362

$$\min \left\{ \sum_{q \in \mathcal{B}_t} a_q \frac{1}{n_q - 1} : \sum_{q \in \mathcal{B}_t} n_q = C, \quad L \leq n_q \leq U, \quad n_q \in \mathbb{R} \forall q \in \mathcal{B}_t \right\}. \quad (8)$$

363
364
365

We can solve (8) efficiently thanks to the next result.

Theorem 5.2 (Continuous allocation, RLOO). *For each $q \in \mathcal{B}_t$, let n_q^* be the function:*

366
367
368
369
370

$$n_q^*(\lambda) = \begin{cases} U & \text{if } \lambda \leq a_q/(U-1)^2, \\ 1 + \sqrt{a_q/\lambda} & \text{if } a_q/(U-1)^2 < \lambda < a_q/(L-1)^2, \\ L & \text{if } \lambda \geq a_q/(L-1)^2 \end{cases} \quad (9)$$

371
372
373

If $BL \leq C \leq BU$, the algebraic equation $\sum_q n_q^*(\lambda^*) = C$ has a unique solution λ^* . Then the unique minimizer of (8) is given by $n_q^* = n_q^*(\lambda^*)$ for all q . Moreover, λ^* can be found by bisection.

374
375
376
377

Heuristic Rounding. First, n_q^* is rounded down to $\lfloor n_q^* \rfloor$. Let $f_q(n)$ denote the per-prompt objective: $f_q(n) = a_q \frac{n-1}{n^2}$ for Dr. GRPO and $f_q(n) = a_q \frac{1}{n-1}$ for RLOO. The remaining budget is then distributed iteratively to prompts with the largest decrease in f_q if an additional rollout is allocated. This process continues until the total budget C is exhausted, while ensuring that the per-prompt bounds, $L \leq \hat{n}_q \leq U$, are satisfied. The procedure is detailed in Appendix D.

378

6 NUMERICAL EXPERIMENTS

381 We now showcase the empirical benefit of our VIP framework on the mathematical reasoning task
 382 and the tool-augmented reasoning task. The common setup for both tasks is as follows: we encode
 383 each prompt q into a 384-dimensional vector x_q using all-MiniLM-L6-v2. Before training,
 384 we pre-compute and cache the pairwise Euclidean distances between all prompt pairs, making the
 385 runtime overhead negligible. We use a median heuristic to set the bandwidth h of the kernel \mathcal{K} . We
 386 also assume that \tilde{Z}_q has the same variances over all q when we compute the allocation; we support
 387 this assumption with a statistical test presented in Appendix B.3. We train all models for one epoch
 388 under two total rollout budgets, $6 \times Q$ and $8 \times Q$, where Q is the dataset size. We integrate VIP on
 389 top of two group-relative policy optimization baselines, RLOO and Dr. GRPO, implemented using
 390 VERL (Sheng et al., 2024) for math experiments and following (Chen et al., 2025b; Jin et al., 2025)
 391 for tool-augmented tasks. We closely follow the default hyperparameter settings used in RL training.
 392 The anonymized repository is <https://anonymous.4open.science/r/VIP-2F00>.

393 **Mathematical Reasoning Task.** For mathematical reasoning, we train on DAPO-MATH-
 394 17k (Yu et al., 2025) and evaluate on AIME2024 and AIME2025. We evaluate VIP by
 395 comparing Dr. GRPO and RLOO, each with and without our adaptive rollout allocation method.
 396 We experiment with three backbone LMs (Qwen2.5-Math-1.5B, Qwen2.5-Math-7B, and
 397 Llama-3.2-3B-Instruct), on AIME24/25, under two rollout-budget settings $C \in \{6 \times Q, 8 \times$
 398 $Q\}$. We report *Pass@32*, *Mean@32*, and *Maj@32* metrics, capturing the accuracy and consensus
 399 of multiple rollouts. We summarize the results in Table 1. Overall, adding VIP yields consistent
 400 improvements on *Pass@32* and *Mean@32* across all three base models and both budgets. For ex-
 401 ample, on Qwen2.5-Math-1.5B at $8 \times Q$, RLOO₊VIP improves *Pass@32* by +12.3 and *Mean@32* by
 402 +6.3 points over RLOO. Similar patterns hold for Llama-3.2-3B-Instruct and Qwen2.5-Math-7B.

403 We see that the relative performance gain from VIP is larger for the 1.5B and 3B models than for the
 404 7B model. This suggests that VIP’s budget-aware variance reduction may particularly help weaker
 405 backbones that otherwise underutilize the rollout budget.

406 **Tool-Augmented Reasoning Task.** We implement our allocation strategy to teach LMs to use a
 407 retrieval tool during generation. We follow Chen et al. (2025b) and train on MuSiQue (19,938
 408 prompts) (Trivedi et al., 2022), evaluating on the Bamboogle benchmark (Press et al., 2022) and
 409 MuSiQue test set. During training we use intfloat/e5-base-v2 embeddings (Wang et al.,
 410 2022) for the retrieval model. We choose Qwen2.5-3B-Instruct as our base model for this
 411 experiment. We use *Precision@5* and *F1@5* to evaluate retrieval quality, and *Exact Match (EM)* for
 412 final generation correctness. We summarize the results in Table 2.

413 Under a fixed rollout budget, VIP improves both answer accuracy and retrieval quality in a *coupled*
 414 manner. On Bamboogle, Dr. GRPO₊VIP raises EM from 20 to 23.2 while simultaneously lifting
 415 *F1@5/Precision@5* by +0.051 / +0.060, and RLOO₊VIP shows larger absolute gains (EM 10.4 →
 416 17.6, *F1@5* 0.190 → 0.264, *Precision@5* 0.225 → 0.294). The parallel improvements in *F1@5*
 417 and *Precision@5* suggest fewer false positives and better ranking of useful contexts, while EM
 418 gains indicate that retrieved evidence is more reliably integrated into final answers. These patterns
 419 support VIP as a sample-efficient, domain-agnostic mechanism for tool-augmented reasoning.

420 **Ablation Studies.** We dissect VIP by ablating its two core components: (i) the *variance predictor*
 421 and (ii) the *adaptive budget allocator*. We replace the Gaussian process predictor (Section 5.1) with
 422 a Ridge Regression baseline and substitute the adaptive allocator (Section 5.2) with two heuristics,
 423 *Inverse Accuracy* and *Inverse Variance* (details in the Appendix). Ablation results on Qwen2.5-
 424 Math-1.5B are summarized in Table 3. RLOO+VIP achieves the best performance across metrics,
 425 outperforming every ablated variants. Among components, *adaptive allocation* is the most critical:
 426 replacing it with heuristics yields substantial drops on all metrics. Substituting the Gaussian pro-
 427 cess with Ridge Regression produces milder but consistent degradations, showing that calibrated
 428 uncertainty further boosts allocation effectiveness. Overall, these results confirm that VIP benefits
 429 primarily from variance-aware budget allocation.

430 **Runtime comparison.** We report the average runtime of each component of our method during a
 431 single gradient step in Table 4. The total computational overhead is extremely small: our method
 432 adds only 1.12% and 0.83% to the overall RL training time for the 1.5B-parameter and 7B-parameter
 433 models, respectively, when including computations cached before training. When excluding cached

432

433
434
435
Table 1: Percentage results on AIME24 and AIME25. The upper block uses a total rollout budget
436
of $C = 8 \times Q$, and the lower block uses $C = 6 \times Q$. For each pair (Dr. GRPO vs Dr. GRPO_{+VIP}
437
and RLOO vs RLOO_{+VIP}), higher values are highlighted in green.

Model	Method	AIME24			AIME25		
		Pass@32	Mean@32	Maj@32	Pass@32	Mean@32	Maj@32
Qwen2.5-Math-1.5B	Dr. GRPO	18.29	4.0	8.81	19.84	2.71	5.81
	Dr. GRPO+VIP	25.0	6.0	13.0	27.0	4.0	9.0
	RLOO	18.29	3.43	6.88	15.90	2.29	8.04
	RLOO+VIP	30.55	9.68	15.65	26.54	6.35	13.72
Qwen2.5-Math-7B	Dr. GRPO	50.0	19.0	34.0	34.0	10.0	15.0
	Dr. GRPO+VIP	58.98	23.65	38.15	36.08	10.0	19.74
	RLOO	53.0	18.0	24.0	45.0	11.0	16.0
	RLOO+VIP	58.0	20.0	35.0	34.0	11.0	18.0
Llama-3.2-3B-Instruct	Dr. GRPO	24.68	6.25	10.62	4.28	0.21	0.07
	Dr. GRPO+VIP	29.18	8.85	17.21	9.37	0.94	2.35
	RLOO	28.84	8.229	13.95	9.157	0.5208	0.3633
	RLOO+VIP	35.59	9.479	19.0	9.99	0.625	0.61
Qwen2.5-Math-1.5B	Dr. GRPO	22.0	4.0	7.0	25.0	3.0	8.0
	Dr. GRPO+VIP	25.0	6.0	13.0	27.0	4.0	9.0
	RLOO	18.0	3.0	7.0	22.0	2.0	3.0
	RLOO+VIP	27.0	6.0	14.0	26.0	8.0	4.0
Qwen2.5-Math-7B	Dr. GRPO	52.0	19.0	35.0	36.0	10.0	20.0
	Dr. GRPO+VIP	57.0	20.0	33.0	36.0	13.0	21.0
	RLOO	37.43	14.79	21.93	41.51	10.0	19.44
	RLOO+VIP	53.85	21.77	35.59	38.32	10.31	21.4
Llama-3.2-3B-Instruct	Dr. GRPO	23.26	6.35	10.09	5.49	0.63	1.31
	Dr. GRPO+VIP	32.34	8.23	14.96	10.67	0.52	0.05
	RLOO	29.3	6.88	1.74	9.57	0.73	1.68
	RLOO+VIP	31.32	7.71	1.77	11.42	0.63	0.32

461
462
463
Table 2: Performance on Bamboogle and MuSiQue. Green cells indicate improvements of the +VIP
464
variant over its base method.

Method	Bamboogle			MuSiQue		
	EM	F1@5	Precision@5	EM	F1@5	Precision@5
Dr. GRPO	20	0.282	0.293	6	0.123	0.126
Dr. GRPO+VIP	23.2	0.333	0.353	10.5	0.214	0.225
RLOO	10.4	0.190	0.225	8.5	0.178	0.179
RLOO+VIP	17.6	0.264	0.294	11	0.209	0.211

473
474
475
Table 3: Ablation study on AIME24 and AIME25. All values are percentages. For each metric, the
476
477
highest value across methods is highlighted in green.

Method	AIME24			AIME25		
	Pass@32	Mean@32	Maj@32	Pass@32	Mean@32	Maj@32
RLOO	18.29	3.43	6.88	15.90	2.29	8.04
RLOO+GP+INVERSE ACC	24.61	6.77	7.90	19.10	3.33	5.03
RLOO+GP+INVERSE VAR	25.83	4.90	10.90	21.11	2.08	3.79
RLOO+RIDGE+ALLOCATION	29.90	6.97	14.79	24.85	5.20	12.12
RLOO+VIP	30.55	9.68	15.65	26.54	6.35	13.72

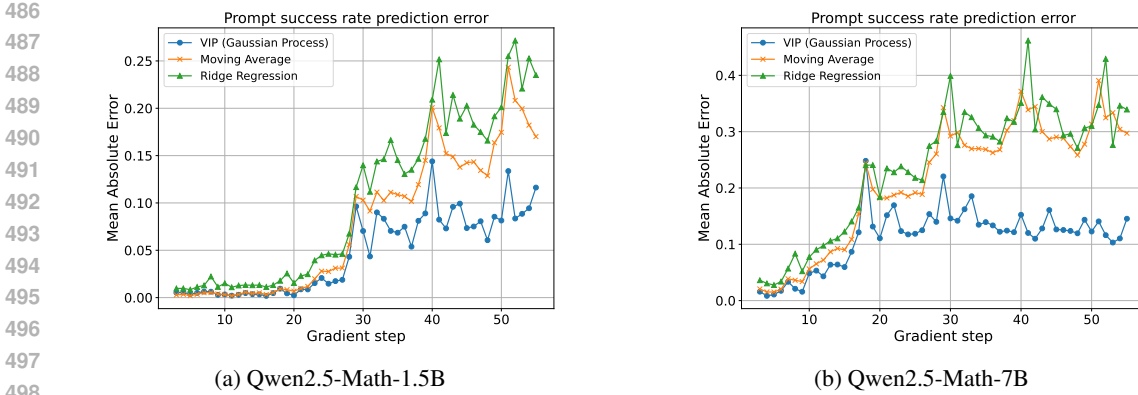


Figure 2: Prediction mean absolute error (MAE) over training steps for two model scales. Our GPR-based predictor achieves consistently lower MAE than moving average and Ridge Regression baselines for both the 1.5B and 7B models.

computations, the overhead further reduces to 0.79% and 0.58%. Because model-forward and rollout costs dominate at larger scales, this relative overhead decreases as model size grows.

Table 4: Wall-clock runtime of core computational components and model-specific operations for Qwen2.5-Math-1.5B and Qwen2.5-Math-7B, measured on a single GPU.

Model	Operation	Time (s)
—	Kernel matrix computation (Algorithm 1)*	10.652
—	Gaussian process training and prediction (Algorithm 1)	0.745
—	Rollout allocation (Section 5.2 + Algorithm 2)	29.956
Qwen2.5-Math-1.5B	Rollout sampling	2781.2
Qwen2.5-Math-1.5B	Log probability computation	627.68
Qwen2.5-Math-1.5B	Policy update	263.9
Qwen2.5-Math-7B	Rollout sampling	3134.4
Qwen2.5-Math-7B	Log probability computation	1388.8
Qwen2.5-Math-7B	Policy update	713.5

*Cached before training.

Success probability prediction quality. To evaluate the quality of our Gaussian Process predictor, we construct a time-series dataset by training Qwen2.5-Math-1.5B and Qwen2.5-Math-7B with RLOO for 55 gradient steps and logging per-prompt success probability at every step. Because the policy changes after each update, the underlying success probabilities drift over time, requiring any predictor to adapt to this non-stationarity. We compare VIP’s GP predictor against two baselines, Moving Average and Ridge Regression, using 1024 most recent samples to predict the next mini-batch’s success probability. Figure 2 reports the MAE across steps. While the Moving Average and Ridge Regression baselines struggle to track rapid changes in model’s behavior, the GP maintains consistently lower MAE throughout training for both model sizes. This indicates that the GP provides a more accurate and adaptive estimator under the non-stationary dynamics of RL training.

7 CONCLUSION

This paper introduced Variance-Informed Predictive allocation, a framework for minimizing gradient variance in group-based reinforcement learning. By combining Gaussian process-based predictions of prompt success probabilities with an optimization approach to rollout allocation, VIP uses limited sampling budgets more efficiently. Our experiments on mathematical reasoning and tool-augmented benchmarks demonstrated consistent gains over heuristic or uniform strategies. VIP is a step toward more adaptive, resource-efficient, and principled training pipelines for large language models. Future work will explore its integration with non-verifiable or noisy rewards, opening avenues for its application in RLHF and other alignment paradigms.

540 **Ethics Statement.** All authors read and agree to adhere to the ICLR Code of Ethics throughout
 541 the development, submission, and potential publication of this work. Our research does not involve
 542 human subjects, personal data, or any sensitive information. All datasets used are publicly available
 543 and do not contain personally identifiable information. We have taken care to ensure that our meth-
 544 ods do not introduce or amplify bias, discrimination, or unfairness, as the reward signals in RLVR
 545 are determined by rule-based verifiers rather than subjective human judgment. We release all code
 546 and experimental protocols to promote transparency and reproducibility. We are not aware of any
 547 potential conflicts of interest, legal compliance issues, or research integrity concerns associated with
 548 this work.

549 **Reproducibility Statement.** We have made every effort to ensure that our results are reproducible.
 550 All of the models, algorithms, and experiments described in the paper are accompanied by detailed
 551 explanations in the main text and appendix. To further support reproducibility, we have provided
 552 an anonymized repository containing the full source code, along with instructions for running the
 553 experiments and replicating our results (see the link in the supplementary materials). The datasets
 554 we used are publicly available, and we include clear descriptions of any preprocessing steps in
 555 the appendix. For all theoretical results, we have stated our assumptions explicitly and included
 556 complete proofs in the supplementary material.

557 **LLM Usage Statement.** In preparing this paper, we used large language models as general-purpose
 558 tools for tasks such as proofreading, rephrasing, and checking the clarity of some sections. The
 559 research ideas, experiments, analysis, and the main writing were carried out by the authors.

560 **REFERENCES**

561 Arash Ahmadian, Chris Cremer, Matthias Gallé, Marzieh Fadaee, Julia Kreutzer, Olivier Pietquin,
 562 Ahmet Üstün, and Sara Hooker. Back to basics: Revisiting reinforce style optimization for learn-
 563 ing from human feedback in LLMs. *arXiv preprint arXiv:2402.14740*, 2024.

564 Jack Chen, Fazhong Liu, Naruto Liu, Yuhan Luo, Erqu Qin, Harry Zheng, Tian Dong, Haojin Zhu,
 565 Yan Meng, and Xiao Wang. Step-wise adaptive integration of supervised fine-tuning and rein-
 566 forcement learning for task-specific llms. *arXiv preprint arXiv:2505.13026*, 2025a.

567 Lichang Chen, Chen Zhu, Davit Soselia, Juhai Chen, Tianyi Zhou, Tom Goldstein, Heng Huang,
 568 Mohammad Shoeybi, and Bryan Catanzaro. Odin: Disentangled reward mitigates hacking in rlhf.
 569 *arXiv preprint arXiv:2402.07319*, 2024.

570 Mingyang Chen, Tianpeng Li, Haoze Sun, Yijie Zhou, Chenzheng Zhu, Haofen Wang, Jeff Z Pan,
 571 Wen Zhang, Huajun Chen, Fan Yang, et al. Learning to reason with search for LLMs via rein-
 572 forcement learning. *arXiv preprint arXiv:2503.19470*, 2025b.

573 Yuqian Fu, Tinghong Chen, Jiajun Chai, Xihuai Wang, Songjun Tu, Guojun Yin, Wei Lin, Qichao
 574 Zhang, Yuanheng Zhu, and Dongbin Zhao. Srft: A single-stage method with supervised and
 575 reinforcement fine-tuning for reasoning. *arXiv preprint arXiv:2506.19767*, 2025.

576 Leo Gao, John Schulman, and Jacob Hilton. Scaling laws for reward model overoptimization. In
 577 *International Conference on Machine Learning*, pp. 10835–10866. PMLR, 2023.

578 Audrey Huang, Wenhao Zhan, Tengyang Xie, Jason D Lee, Wen Sun, Akshay Krishnamurthy, and
 579 Dylan J Foster. Correcting the mythos of kl-regularization: Direct alignment without overopti-
 580 mization via chi-squared preference optimization. *arXiv preprint arXiv:2407.13399*, 2024.

581 Jiajie Jin, Yutao Zhu, Zhicheng Dou, Guanting Dong, Xinyu Yang, Chenghao Zhang, Tong Zhao,
 582 Zhao Yang, and Ji-Rong Wen. Flashrag: A modular toolkit for efficient retrieval-augmented
 583 generation research. In *Companion Proceedings of the ACM on Web Conference 2025*, pp. 737–
 584 740, 2025.

585 Deyang Kong, Qi Guo, Xiangyu Xi, Wei Wang, Jingang Wang, Xunliang Cai, Shikun Zhang,
 586 and Wei Ye. Rethinking the sampling criteria in reinforcement learning for llm reasoning: A
 587 competence-difficulty alignment perspective. *arXiv preprint arXiv:2505.17652*, 2025.

588 Cassidy Laidlaw, Shivam Singhal, and Anca Dragan. Correlated proxies: A new definition and
 589 improved mitigation for reward hacking. *arXiv preprint arXiv:2403.03185*, 2024.

594 Min Lee, Jinsu Kim, Seongmin Park, Young Choi, Sungmin Jung, and Sangjun Han. MaxInfoRL:
 595 Boosting exploration in reinforcement learning through information gain maximization. *arXiv*
 596 *preprint arXiv:2412.12098*, 2024.

597

598 Mengqi Liao, Xiangyu Xi, Chen Ruinian, Jia Leng, Yangen Hu, Ke Zeng, Shuai Liu, and Huaiyu
 599 Wan. Enhancing efficiency and exploration in reinforcement learning for llms. In *Proceedings*
 600 *of the 2025 Conference on Empirical Methods in Natural Language Processing*, pp. 1451–1463,
 601 2025.

602 Zhihang Lin, Mingbao Lin, Yuan Xie, and Rongrong Ji. Cppo: Accelerating the training of group
 603 relative policy optimization-based reasoning models. *arXiv preprint arXiv:2503.22342*, 2025.

604

605 Zichen Liu, Changyu Chen, Wenjun Li, Penghui Qi, Tianyu Pang, Chao Du, Wee Sun Lee,
 606 and Min Lin. Understanding r1-zero-like training: A critical perspective. *arXiv preprint*
 607 *arXiv:2503.20783*, 2025.

608 Ofir Press, Muru Zhang, Sewon Min, Ludwig Schmidt, Noah A Smith, and Mike Lewis. Measuring
 609 and narrowing the compositionality gap in language models. *arXiv preprint arXiv:2210.03350*,
 610 2022.

611

612 Alexandre Ramé, Nino Vieillard, Léonard Hussenot, Robert Dadashi, Geoffrey Cideron, Olivier
 613 Bachem, and Johan Ferret. Warm: On the benefits of weight averaged reward models. *arXiv*
 614 *preprint arXiv:2401.12187*, 2024.

615

616 John Schulman, Sergey Levine, Pieter Abbeel, Michael Jordan, and Philipp Moritz. Trust region
 617 policy optimization. In *International Conference on Machine Learning*, pp. 1889–1897. PMLR,
 618 2015.

619 Zhihong Shao, Peiyi Wang, Qihao Zhu, Runxin Xu, Junxiao Song, Xiao Bi, Haowei Zhang,
 620 Mingchuan Zhang, YK Li, Yang Wu, et al. Deepseekmath: Pushing the limits of mathematical
 621 reasoning in open language models. *arXiv preprint arXiv:2402.03300*, 2024.

622

623 Guangming Sheng, Chi Zhang, Zilingfeng Ye, Xibin Wu, Wang Zhang, Ru Zhang, Yanghua Peng,
 624 Haibin Lin, and Chuan Wu. Hybridflow: A flexible and efficient RLHF framework. *arXiv preprint*
 625 *arXiv: 2409.19256*, 2024.

626

627 Joar Skalse, Nikolaus Howe, Dmitrii Krasheninnikov, and David Krueger. Defining and character-
 628 izing reward gaming. *Advances in Neural Information Processing Systems*, 35:9460–9471, 2022.

629

630 Yuda Song, Gokul Swamy, Aarti Singh, J Bagnell, and Wen Sun. The importance of online data:
 631 Understanding preference fine-tuning via coverage. *Advances in Neural Information Processing*
 632 *Systems*, 37:12243–12270, 2024.

633

634 Yifan Sun, Jingyan Shen, Yibin Wang, Tianyu Chen, Zhendong Wang, Mingyuan Zhou, and Huan
 635 Zhang. Improving data efficiency for llm reinforcement fine-tuning through difficulty-targeted
 636 online data selection and rollout replay. *arXiv preprint arXiv:2506.05316*, 2025.

637

638 Harsh Trivedi, Niranjan Balasubramanian, Tushar Khot, and Ashish Sabharwal. Musique: Multihop
 639 questions via single-hop question composition. *Transactions of the Association for Computational*
 640 *Linguistics*, 10:539–554, 2022.

641

642 Liang Wang, Nan Yang, Xiaolong Huang, Binxing Jiao, Linjun Yang, Dixin Jiang, Rangan Ma-
 643 jumder, and Furu Wei. Text embeddings by weakly-supervised contrastive pre-training. *arXiv*
 644 *preprint arXiv:2212.03533*, 2022.

645

646 Yixuan Even Xu, Yash Savani, Fei Fang, and J Zico Kolter. Not all rollouts are useful: Down-
 647 sampling rollouts in llm reinforcement learning. *arXiv preprint arXiv:2504.13818*, 2025.

648

649 Zhicheng Yang, Zhijiang Guo, Yinya Huang, Yongxin Wang, Dongchun Xie, Yiwei Wang, Xiaodan
 650 Liang, and Jing Tang. Depth-breadth synergy in rlrv: Unlocking llm reasoning gains with adaptive
 651 exploration. *arXiv preprint arXiv:2508.13755*, 2025.

648 Qiying Yu, Zheng Zhang, Ruofei Zhu, Yufeng Yuan, Xiaochen Zuo, Yu Yue, Weinan Dai, Tiantian
649 Fan, Gaohong Liu, Lingjun Liu, et al. Dapo: An open-source LLM reinforcement learning system
650 at scale. *arXiv preprint arXiv:2503.14476*, 2025.

651 Ruiqi Zhang, Daman Arora, Song Mei, and Andrea Zanette. Speed-rl: Faster training of reasoning
652 models via online curriculum learning. *arXiv preprint arXiv:2506.09016*, 2025.

653 Haizhong Zheng, Yang Zhou, Brian R Bartoldson, Bhavya Kailkhura, Fan Lai, Jiawei Zhao, and
654 Beidi Chen. Act only when it pays: Efficient reinforcement learning for llm reasoning via selective
655 rollouts. *arXiv preprint arXiv:2506.02177*, 2025.

656

657

658

659

660

661

662

663

664

665

666

667

668

669

670

671

672

673

674

675

676

677

678

679

680

681

682

683

684

685

686

687

688

689

690

691

692

693

694

695

696

697

698

699

700

701

A PROOFS OF TECHNICAL RESULTS

A.1 PROOFS OF SECTION 4

Proof of Proposition 4.2. We recall the expression of \tilde{G}_q :

$$\tilde{G}_q = \frac{1}{n} \sum_{j=1}^n (\tilde{R}_j - \frac{1}{n} \sum_{k=1}^n \tilde{R}_k) \tilde{Z}_j.$$

The expectation of \tilde{G}_q is:

$$\begin{aligned} \mathbb{E}[\tilde{G}_q] &= \mathbb{E}\left[\frac{1}{n} \sum_{j=1}^n (\tilde{R}_j - \frac{1}{n} \sum_{k=1}^n \tilde{R}_k) \tilde{Z}_j\right] \\ &= \mathbb{E}\left[\frac{1}{n} \sum_{j=1}^n \tilde{R}_j \tilde{Z}_j - \frac{1}{n^2} \sum_{j=1}^n \sum_{k=1}^n \tilde{R}_k \tilde{Z}_j\right] \\ &= \frac{1}{n} \sum_{j=1}^n \mathbb{E}[\tilde{R}_j \tilde{Z}_j] - \frac{1}{n^2} \sum_{j=1}^n \sum_{k=1}^n \mathbb{E}[\tilde{R}_k \tilde{Z}_j] \\ &= \mathbb{E}[\tilde{R} \tilde{Z}] - \mathbb{E}[\tilde{R} \tilde{Z}] = 0 \quad (\text{by Assumption 4.1(i)}). \end{aligned}$$

The variance of \tilde{G}_q is:

$$\begin{aligned} \text{Var}(\tilde{G}_q) &= \mathbb{E}[\tilde{G}_q^2] - (\mathbb{E}[\tilde{G}_q])^2 = \mathbb{E}[\tilde{G}_q^2] - 0 = \mathbb{E}[\tilde{G}_q^2] \\ &= \mathbb{E}\left[\left(\frac{1}{n} \sum_{j=1}^n \tilde{R}_j \tilde{Z}_j - \frac{1}{n^2} \sum_{j=1}^n \sum_{k=1}^n \tilde{R}_k \tilde{Z}_j\right)^2\right] \\ &= \mathbb{E}\left[\frac{1}{n^2} \left(\sum_{j=1}^n \tilde{R}_j \tilde{Z}_j\right)^2 + \frac{1}{n^4} \left(\sum_{j=1}^n \sum_{k=1}^n \tilde{R}_k \tilde{Z}_j\right)^2 - \frac{2}{n^3} \left(\sum_{j=1}^n \tilde{R}_j \tilde{Z}_j\right) \left(\sum_{j=1}^n \sum_{k=1}^n \tilde{R}_k \tilde{Z}_j\right)\right] \\ &= \underbrace{\mathbb{E}\left[\frac{1}{n^2} \left(\sum_{j=1}^n \tilde{R}_j \tilde{Z}_j\right)^2\right]}_{\triangleq C_1} + \underbrace{\mathbb{E}\left[\frac{1}{n^4} \left(\sum_{j=1}^n \sum_{k=1}^n \tilde{R}_k \tilde{Z}_j\right)^2\right]}_{\triangleq C_2} - \underbrace{\mathbb{E}\left[\frac{2}{n^3} \left(\sum_{j=1}^n \tilde{R}_j \tilde{Z}_j\right) \left(\sum_{j=1}^n \sum_{k=1}^n \tilde{R}_k \tilde{Z}_j\right)\right]}_{\triangleq C_3}. \end{aligned}$$

756 Next we compute each term. We find for C_1 :

$$\begin{aligned}
 C_1 &= \mathbb{E} \left[\frac{1}{n^2} \left(\sum_{j=1}^n \tilde{R}_j \tilde{Z}_j \right)^2 \right] = \frac{1}{n^2} \mathbb{E} \left[\left(\sum_{j=1}^n \tilde{R}_j \tilde{Z}_j \right)^2 \right] \\
 &= \frac{1}{n^2} \mathbb{E} \left[\sum_{j=1}^n \tilde{R}_j^2 \tilde{Z}_j^2 + \sum_{1 \leq j < k \leq n} \tilde{R}_j \tilde{Z}_j \tilde{R}_k \tilde{Z}_k \right] \\
 &= \frac{1}{n^2} \left(\sum_{j=1}^n \mathbb{E} [\tilde{R}_j^2 \tilde{Z}_j^2] + \sum_{1 \leq j < k \leq n} \mathbb{E} [\tilde{R}_j \tilde{Z}_j \tilde{R}_k \tilde{Z}_k] \right) \\
 &= \frac{1}{n^2} \left(\sum_{j=1}^n \mathbb{E} [\tilde{R}_j^2 \tilde{Z}_j^2] + \sum_{1 \leq j < k \leq n} \mathbb{E} [\tilde{R}_j \tilde{Z}_j] \mathbb{E} [\tilde{R}_k \tilde{Z}_k] \right) \quad (\text{independence between } j \text{ and } k) \\
 &= \frac{1}{n^2} \left(n \mathbb{E} [\tilde{R}^2 \tilde{Z}^2] + n(n-1) (\mathbb{E} [\tilde{R} \tilde{Z}])^2 \right) \quad (\text{identically distributed}) \\
 &= \frac{1}{n} \mathbb{E} [\tilde{R}^2 \tilde{Z}^2] + \frac{(n-1)}{n} (\mathbb{E} [\tilde{R} \tilde{Z}])^2 \\
 &= \frac{1}{n} \mathbb{E} [\tilde{R}^2] (\mu_Z^2 + \sigma_Z^2) + \frac{n-1}{n} \mu_z^2 (\mathbb{E} [\tilde{R}])^2 \\
 &= \mathbb{E} [\tilde{R}^2] \left(\frac{1}{n} \mu_Z^2 + \frac{1}{n} \sigma_Z^2 \right) + (\mathbb{E} [\tilde{R}])^2 \left(\frac{n-1}{n} \mu_z^2 \right).
 \end{aligned}$$

781 We next compute for C_2 :

$$C_2 = \mathbb{E} \left[\frac{1}{n^4} \left(\sum_{j=1}^n \sum_{k=1}^n \tilde{R}_k \tilde{Z}_j \right)^2 \right] = \frac{1}{n^4} \mathbb{E} \left[\sum_{k=1}^n \sum_{k'=1}^n \sum_{j=1}^n \sum_{j'=1}^n \tilde{R}_k \tilde{R}_{k'} \tilde{Z}_j \tilde{Z}_{j'} \right].$$

787 We can decompose the quadruple sum by whether the indices are equal or not. There are four
788 index-pattern types:

- 791 • When $k = k'$ and $j = j'$: there are n^2 such terms, each term is $\mathbb{E} [\tilde{R}^2 \tilde{Z}^2] = (\mu_Z^2 + \sigma_Z^2) \mathbb{E} [\tilde{R}^2]$.
792 Total contribution to C_2 is

$$T_1 = n^2 (\mu_Z^2 + \sigma_Z^2) \mathbb{E} [\tilde{R}^2].$$

- 795 • When $k = k'$ and $j \neq j'$: there are $n^2(n-1)$ such terms. For any fixed k and distinct j, j' ,
796 $\mathbb{E} [\tilde{R}_k^2 \tilde{Z}_j \tilde{Z}_{j'}] = \mathbb{E} [\tilde{R}_k^2] \mathbb{E} [\tilde{Z}_j \tilde{Z}_{j'}] = \mu_Z^2 \mathbb{E} [\tilde{R}^2]$. Total contribution to C_2 is

$$T_2 = n^2(n-1) \mu_Z^2 \mathbb{E} [\tilde{R}^2].$$

- 801 • When $k \neq k'$ and $j = j'$: there are $n^2(n-1)$ such terms. For distinct k, k' , $\mathbb{E} [\tilde{R}_k \tilde{R}_{k'} \tilde{Z}^2] =$
802 $\mathbb{E} [\tilde{R}_k \tilde{R}_{k'}] \mathbb{E} [\tilde{Z}^2] = (\mu_Z^2 + \sigma_Z^2) (\mathbb{E} [\tilde{R}])^2$. Total contribution to C_2 is

$$T_3 = n^2(n-1) (\mu_Z^2 + \sigma_Z^2) (\mathbb{E} [\tilde{R}])^2.$$

- 856 • When $k \neq k'$ and $j \neq j'$: there are $n^2(n-1)^2$ such terms. For all indices different,
857 $\mathbb{E} [\tilde{R}_k \tilde{R}_{k'} \tilde{Z}_j \tilde{Z}_{j'}] = \mu_Z^2 (\mathbb{E} [\tilde{R}])^2$. Total contribution to C_2 is

$$T_4 = n^2(n-1)^2 \mu_Z^2 (\mathbb{E} [\tilde{R}])^2.$$

810 Therefore, we find
 811

$$\begin{aligned}
 C_2 &= \frac{1}{n^4} (T_1 + T_2 + T_3 + T_4) \\
 &= \frac{1}{n^4} \left[n^2(\mu_Z^2 + \sigma_Z^2) \mathbb{E}[\tilde{R}^2] + n^2(n-1)\mu_Z^2 \mathbb{E}[\tilde{R}^2] \right. \\
 &\quad \left. + n^2(n-1)(\mu_Z^2 + \sigma_Z^2)(\mathbb{E}[\tilde{R}])^2 + n^2(n-1)^2\mu_Z^2(\mathbb{E}[\tilde{R}])^2 \right] \\
 &= \mathbb{E}[\tilde{R}^2] \left(\frac{\mu_Z^2}{n} + \frac{\sigma_Z^2}{n^2} \right) + (\mathbb{E}[\tilde{R}])^2 \left(\frac{n-1}{n} \mu_Z^2 + \frac{n-1}{n^2} \sigma_Z^2 \right).
 \end{aligned}$$

820 We next compute for C_3 :

$$C_3 = \mathbb{E} \left[\frac{2}{n^3} \left(\sum_{j=1}^n \tilde{R}_j \tilde{Z}_j \right) \left(\sum_{j'=1}^n \sum_{k=1}^n \tilde{R}_k \tilde{Z}_{j'} \right) \right] = \frac{2}{n^3} \mathbb{E} \left[\sum_{j=1}^n \sum_{j'=1}^n \sum_{k=1}^n \tilde{R}_j \tilde{Z}_j \tilde{R}_k \tilde{Z}_{j'} \right].$$

825 We can decompose the triplet sum by whether the indices are equal or not. There are five index-
 826 pattern types:

827 • When $j = k = j'$: there are n such terms. For each j , $\mathbb{E}[\tilde{R}_j^2 \tilde{Z}_j^2] = \mathbb{E}[\tilde{R}_j^2] \mathbb{E}[\tilde{Z}_j^2] = (\mu_Z^2 + \sigma_Z^2) \mathbb{E}[\tilde{R}^2]$. Total contribution:

$$T_1 = n(\mu_Z^2 + \sigma_Z^2) \mathbb{E}[\tilde{R}^2].$$

830 • When $j = k \neq j'$: there are $n(n-1)$ such terms. For each j and $j' \neq j$, $\mathbb{E}[\tilde{R}_j^2 \tilde{Z}_j \tilde{Z}_{j'}] = \mathbb{E}[\tilde{R}_j^2] \mathbb{E}[\tilde{Z}_j \tilde{Z}_{j'}] = \mathbb{E}[\tilde{R}^2] \mathbb{E}[\tilde{Z}_j] \mathbb{E}[\tilde{Z}_{j'}] = \mathbb{E}[\tilde{R}^2] \mu_Z^2$. Total contribution is

$$T_2 = n(n-1) \mathbb{E}[\tilde{R}^2] \mu_Z^2.$$

834 • When $j = j' \neq k$: there are $n(n-1)$ such terms. For each j and $k \neq j$, $\mathbb{E}[\tilde{R}_j \tilde{Z}_j^2 \tilde{R}_k] = \mathbb{E}[\tilde{R}_j \tilde{R}_k] \mathbb{E}[\tilde{Z}_j^2] = (\mu_Z^2 + \sigma_Z^2)(\mathbb{E}[\tilde{R}])^2$. Total contribution is

$$T_3 = n(n-1)(\mu_Z^2 + \sigma_Z^2)(\mathbb{E}[\tilde{R}])^2.$$

839 • When $k = j' \neq j$: there are $n(n-1)$ such terms. For each j and $k \neq j$, $\mathbb{E}[\tilde{R}_j \tilde{Z}_j \tilde{R}_k \tilde{Z}_k] = \mathbb{E}[\tilde{R}_j \tilde{R}_k] \mathbb{E}[\tilde{Z}_j \tilde{Z}_k] = \mu_Z^2 (\mathbb{E}[\tilde{R}])^2$. Total contribution is

$$T_4 = n(n-1) \mu_Z^2 (\mathbb{E}[\tilde{R}])^2.$$

844 • When j, j', k are all distinct: there are $n(n-1)(n-2)$ such terms. For each triple of distinct
 845 indices, $\mathbb{E}[\tilde{R}_j \tilde{Z}_j \tilde{R}_k \tilde{Z}_{j'}] = \mu_Z^2 (\mathbb{E}[\tilde{R}])^2$. Total contribution is

$$T_5 = n(n-1)(n-2) \mu_Z^2 (\mathbb{E}[\tilde{R}])^2.$$

850 Therefore, we find
 851

$$\begin{aligned}
 C_3 &= \frac{2}{n^3} (T_1 + T_2 + T_3 + T_4 + T_5) \\
 &= \frac{2}{n^3} \left[n(\mu_Z^2 + \sigma_Z^2) \mathbb{E}[\tilde{R}^2] + n(n-1) \mathbb{E}[\tilde{R}^2] \mu_Z^2 \right. \\
 &\quad \left. + n(n-1)(\mu_Z^2 + \sigma_Z^2) (\mathbb{E}[\tilde{R}])^2 + n(n-1) \mu_Z^2 (\mathbb{E}[\tilde{R}])^2 \right. \\
 &\quad \left. + n(n-1)(n-2) \mu_Z^2 (\mathbb{E}[\tilde{R}])^2 \right] \\
 &= \mathbb{E}[\tilde{R}^2] \left(\frac{2}{n} \mu_Z^2 + \frac{2}{n^2} \sigma_Z^2 \right) + (\mathbb{E}[\tilde{R}])^2 \left(\frac{2n-2}{n} \mu_Z^2 + \frac{2n-2}{n^2} \sigma_Z^2 \right).
 \end{aligned}$$

864 Group terms with $\mathbb{E}[\tilde{R}^2]$ and $(\mathbb{E}[\tilde{R}])^2$ coefficients:

$$865 \quad C_1 + C_2 - C_3 = \mathbb{E}[\tilde{R}^2] \left[\left(\frac{1}{n} \mu_Z^2 + \frac{1}{n} \sigma_Z^2 \right) + \left(\frac{\mu_Z^2}{n} + \frac{\sigma_Z^2}{n^2} \right) - \left(\frac{2}{n} \mu_Z^2 + \frac{2}{n^2} \sigma_Z^2 \right) \right] \\ 866 \quad + (\mathbb{E}[\tilde{R}])^2 \left[\frac{n-1}{n} \mu_Z^2 + \left(\frac{n-1}{n} \mu_Z^2 + \frac{n-1}{n^2} \sigma_Z^2 \right) - \left(\frac{2n-2}{n} \mu_Z^2 + \frac{2n-2}{n^2} \sigma_Z^2 \right) \right]. \\ 867$$

871 We simplify each bracket to obtain:

$$872 \quad \text{Var}(\tilde{G}_q) = C_1 + C_2 - C_3 = \frac{n-1}{n^2} \sigma_Z^2 \left(\mathbb{E}[\tilde{R}^2] - (\mathbb{E}[\tilde{R}])^2 \right) = \frac{n-1}{n^2} \sigma_Z^2 \sigma_R^2. \\ 873$$

874 For a given prompt, \tilde{R} takes 1 with probability p and -1 with probability $1-p$, leading to its
875 variance of $4p(1-p)$. We obtain the final variance of the per-prompt gradient estimator:

$$876 \quad \text{Var}(\tilde{G}_q) = \frac{\sigma_Z^2(n-1)}{n^2} \cdot 4p(1-p). \\ 877$$

878 This completes the proof. \square

880 *Proof of Proposition 4.3.* We recall the expression of \tilde{G}_q :

$$881 \quad \tilde{G}_q = \frac{1}{n} \sum_{j=1}^n \left(\tilde{R}_j - \frac{1}{n-1} \sum_{\substack{k=1 \\ k \neq j}}^n \tilde{R}_k \right) \tilde{Z}_j.$$

885 The expectation of \tilde{G}_q is:

$$886 \quad \mathbb{E}[\tilde{G}_q] = \mathbb{E} \left[\frac{1}{n} \sum_{j=1}^n \left(\tilde{R}_j - \frac{1}{n-1} \sum_{\substack{k=1 \\ k \neq j}}^n \tilde{R}_k \right) \tilde{Z}_j \right] \\ 887 \\ 888 \quad = \mathbb{E} \left[\frac{1}{n} \sum_{j=1}^n \tilde{R}_j \tilde{Z}_j - \frac{1}{n(n-1)} \sum_{j=1}^n \sum_{\substack{k=1 \\ k \neq j}}^n \tilde{R}_k \tilde{Z}_j \right] \\ 889 \\ 890 \quad = \frac{1}{n} \sum_{j=1}^n \mathbb{E}[\tilde{R}_j \tilde{Z}_j] - \frac{1}{n(n-1)} \sum_{j=1}^n \sum_{\substack{k=1 \\ k \neq j}}^n \mathbb{E}[\tilde{R}_k \tilde{Z}_j] \\ 891 \\ 892 \quad = \mathbb{E}[\tilde{R} \tilde{Z}] - \mathbb{E}[\tilde{R} \tilde{Z}] \\ 893 \\ 894 \quad = 0. \quad (\text{by Assumption 4.1(i)}) \\ 895 \\ 896$$

901 The variance of \tilde{G}_q is:

$$902 \quad \text{Var}(\tilde{G}_q) \\ 903 \quad = \mathbb{E}[\tilde{G}_q^2] - (\mathbb{E}[\tilde{G}_q])^2 = \mathbb{E}[\tilde{G}_q^2] - 0 = \mathbb{E}[\tilde{G}_q^2] \\ 904 \\ 905 \quad = \mathbb{E} \left[\left(\frac{1}{n} \sum_{j=1}^n \tilde{R}_j \tilde{Z}_j - \frac{1}{n(n-1)} \sum_{j=1}^n \sum_{\substack{k=1 \\ k \neq j}}^n \tilde{R}_k \tilde{Z}_j \right)^2 \right] \\ 906 \\ 907 \quad = \mathbb{E} \left[\frac{1}{n^2} \left(\sum_{j=1}^n \tilde{R}_j \tilde{Z}_j \right)^2 + \frac{1}{n^2(n-1)^2} \left(\sum_{j=1}^n \sum_{\substack{k=1 \\ k \neq j}}^n \tilde{R}_k \tilde{Z}_j \right)^2 - \frac{2}{n^2(n-1)} \left(\sum_{j=1}^n \tilde{R}_j \tilde{Z}_j \right) \left(\sum_{j=1}^n \sum_{\substack{k=1 \\ k \neq j}}^n \tilde{R}_k \tilde{Z}_j \right) \right] \\ 908 \\ 909 \quad = \mathbb{E} \underbrace{\left[\frac{1}{n^2} \left(\sum_{j=1}^n \tilde{R}_j \tilde{Z}_j \right)^2 \right]}_{\triangleq C_1} + \mathbb{E} \underbrace{\left[\frac{1}{n^2(n-1)^2} \left(\sum_{j=1}^n \sum_{\substack{k=1 \\ k \neq j}}^n \tilde{R}_k \tilde{Z}_j \right)^2 \right]}_{\triangleq C_2} - \mathbb{E} \underbrace{\left[\frac{2}{n^2(n-1)} \left(\sum_{j=1}^n \tilde{R}_j \tilde{Z}_j \right) \left(\sum_{j=1}^n \sum_{\substack{k=1 \\ k \neq j}}^n \tilde{R}_k \tilde{Z}_j \right) \right]}_{\triangleq C_3}.$$

918 The first term C_1 is already computed in the proof of Proposition 4.2, and we have:
919

$$920 \quad C_1 = \mathbb{E}[\tilde{R}^2] \left(\frac{1}{n} \mu_Z^2 + \frac{1}{n} \sigma_Z^2 \right) + (\mathbb{E}[\tilde{R}])^2 \left(\frac{n-1}{n} \mu_Z^2 \right).$$

922 Next, we consider the term C_2 :
923

$$\begin{aligned} 924 \quad C_2 &= \mathbb{E} \left[\frac{1}{n^2(n-1)^2} \left(\sum_{j=1}^n \sum_{\substack{k=1 \\ k \neq j}}^n \tilde{R}_k \tilde{Z}_j \right)^2 \right] \\ 925 \\ 926 \\ 927 \\ 928 \quad &= \mathbb{E} \left[\frac{1}{n^2(n-1)^2} \left(\left(\sum_{j=1}^n \sum_{k=1}^n \tilde{R}_k \tilde{Z}_j \right) - \left(\sum_{j=1}^n \tilde{R}_j \tilde{Z}_j \right) \right)^2 \right] \\ 929 \\ 930 \\ 931 \\ 932 \quad &= \frac{1}{n^2(n-1)^2} \left(\mathbb{E} \left[\left(\sum_{j=1}^n \sum_{k=1}^n \tilde{R}_k \tilde{Z}_j \right)^2 \right] - 2 \mathbb{E} \left[\left(\sum_{j=1}^n \sum_{k=1}^n \tilde{R}_k \tilde{Z}_j \right) \left(\sum_{j'=1}^n \tilde{R}_{j'} \tilde{Z}_{j'} \right) \right] + \mathbb{E} \left[\left(\sum_{j=1}^n \tilde{R}_j \tilde{Z}_j \right)^2 \right] \right). \\ 933 \\ 934 \\ 935 \end{aligned}$$

936 We can utilize the computation from the proof of Proposition 4.2 to have:
937

$$\begin{aligned} 938 \quad \mathbb{E} \left[\frac{1}{n^4} \left(\sum_{j=1}^n \sum_{k=1}^n \tilde{R}_k \tilde{Z}_j \right)^2 \right] &= \mathbb{E}[\tilde{R}^2] \left(\frac{\mu_Z^2}{n} + \frac{\sigma_Z^2}{n^2} \right) + (\mathbb{E}[\tilde{R}])^2 \left(\frac{n-1}{n} \mu_Z^2 + \frac{n-1}{n^2} \sigma_Z^2 \right), \\ 939 \\ 940 \\ 941 \quad \mathbb{E} \left[\frac{2}{n^3} \left(\sum_{j=1}^n \tilde{R}_j \tilde{Z}_j \right) \left(\sum_{j'=1}^n \sum_{k=1}^n \tilde{R}_k \tilde{Z}_{j'} \right) \right] &= \mathbb{E}[\tilde{R}^2] \left(\frac{2}{n} \mu_Z^2 + \frac{2}{n^2} \sigma_Z^2 \right) + (\mathbb{E}[\tilde{R}])^2 \left(\frac{2n-2}{n} \mu_Z^2 + \frac{2n-2}{n^2} \sigma_Z^2 \right), \\ 942 \\ 943 \\ 944 \quad \mathbb{E} \left[\frac{1}{n^2} \left(\sum_{j=1}^n \tilde{R}_j \tilde{Z}_j \right)^2 \right] &= \mathbb{E}[\tilde{R}^2] \left(\frac{1}{n} \mu_Z^2 + \frac{1}{n} \sigma_Z^2 \right) + (\mathbb{E}[\tilde{R}])^2 \left(\frac{n-1}{n} \mu_Z^2 \right). \\ 945 \\ 946 \\ 947 \end{aligned}$$

948 Therefore,
949

$$\begin{aligned} 950 \quad C_2 &= \mathbb{E}[\tilde{R}^2] \left[\frac{n}{(n-1)^2} \mu_Z^2 + \frac{1}{(n-1)^2} \sigma_Z^2 - \left(\frac{2}{(n-1)^2} \mu_Z^2 + \frac{2}{n(n-1)^2} \sigma_Z^2 \right) + \frac{1}{n(n-1)^2} \mu_Z^2 + \frac{1}{n(n-1)^2} \sigma_Z^2 \right] \\ 951 \\ 952 \\ 953 \quad + (\mathbb{E}[\tilde{R}])^2 \left[\frac{n}{(n-1)} \mu_Z^2 + \frac{1}{(n-1)} \sigma_Z^2 - \left(\frac{2}{n-1} \mu_Z^2 + \frac{2}{n(n-1)} \sigma_Z^2 \right) + \frac{1}{n(n-1)} \mu_Z^2 \right] \\ 954 \\ 955 \quad = \mathbb{E}[\tilde{R}^2] \left[\frac{n^2-2n+1}{n(n-1)^2} \mu_Z^2 + \frac{n-1}{n(n-1)^2} \sigma_Z^2 \right] + (\mathbb{E}[\tilde{R}])^2 \left[\frac{n^2-2n+1}{n(n-1)} \mu_Z^2 + \frac{n-2}{n(n-1)} \sigma_Z^2 \right] \\ 956 \\ 957 \\ 958 \quad = \mathbb{E}[\tilde{R}^2] \left[\frac{1}{n} \mu_Z^2 + \frac{1}{n(n-1)} \sigma_Z^2 \right] + (\mathbb{E}[\tilde{R}])^2 \left[\frac{n-1}{n} \mu_Z^2 + \frac{n-2}{n(n-1)} \sigma_Z^2 \right]. \\ 959 \\ 960 \end{aligned}$$

961 We compute C_3 as follows:
962

$$\begin{aligned} 963 \quad C_3 &= \mathbb{E} \left[\frac{2}{n^2(n-1)} \left(\sum_{j=1}^n \tilde{R}_j \tilde{Z}_j \right) \left(\sum_{j'=1}^n \sum_{\substack{k=1 \\ k \neq j'}}^n \tilde{R}_k \tilde{Z}_{j'} \right) \right] \\ 964 \\ 965 \\ 966 \quad &= \mathbb{E} \left[\frac{2}{n^2(n-1)} \left(\sum_{j=1}^n \tilde{R}_j \tilde{Z}_j \right) \left(\sum_{j'=1}^n \sum_{k=1}^n \tilde{R}_k \tilde{Z}_{j'} - \sum_{j'=1}^n \tilde{R}_{j'} \tilde{Z}_{j'} \right) \right] \\ 967 \\ 968 \\ 969 \quad &= \frac{2}{n^2(n-1)} \left(\mathbb{E} \left[\left(\sum_{j=1}^n \tilde{R}_j \tilde{Z}_j \right) \left(\sum_{j'=1}^n \sum_{k=1}^n \tilde{R}_k \tilde{Z}_{j'} \right) \right] - \mathbb{E} \left[\left(\sum_{j=1}^n \tilde{R}_j \tilde{Z}_j \right) \left(\sum_{j'=1}^n \tilde{R}_{j'} \tilde{Z}_{j'} \right) \right] \right). \\ 970 \\ 971 \end{aligned}$$

972 We can utilize the computation of $\frac{n^3}{2}C_3$ and n^2C_1 from the proof of Proposition 4.2 to have:
973

$$974 \mathbb{E} \left[\left(\sum_{j=1}^n \tilde{R}_j \tilde{Z}_j \right) \left(\sum_{j'=1}^n \sum_{k=1}^n \tilde{R}_k \tilde{Z}_{j'} \right) \right] = \mathbb{E}[\tilde{R}^2] (n^2 \mu_Z^2 + n \sigma_Z^2) + (\mathbb{E}[\tilde{R}])^2 (n^2(n-1) \mu_Z^2 + n(n-1) \sigma_Z^2), \\ 975 \\ 976 \mathbb{E} \left[\left(\sum_{j=1}^n \tilde{R}_j \tilde{Z}_j \right) \left(\sum_{j'=1}^n \tilde{R}_{j'} \tilde{Z}_{j'} \right) \right] = \mathbb{E}[\tilde{R}^2] (n \mu_Z^2 + n \sigma_Z^2) + (\mathbb{E}[\tilde{R}])^2 (n(n-1) \mu_Z^2).$$

977 Plugging these terms to the computation of C_3 yields us:
978

$$979 C_3 = \frac{2}{n^2(n-1)} \left\{ \mathbb{E}[\tilde{R}^2] (n^2 \mu_Z^2 + n \sigma_Z^2) + (\mathbb{E}[\tilde{R}])^2 (n^2(n-1) \mu_Z^2 + n(n-1) \sigma_Z^2) \right. \\ 980 \left. - \left[\mathbb{E}[\tilde{R}^2] (n \mu_Z^2 + n \sigma_Z^2) + (\mathbb{E}[\tilde{R}])^2 (n(n-1) \mu_Z^2) \right] \right\} \\ 981 \\ 982 = \mathbb{E}[\tilde{R}^2] \cdot \frac{2(n^2 - n)}{n^2(n-1)} \mu_Z^2 + (\mathbb{E}[\tilde{R}])^2 \cdot \frac{2n(n-1)}{n^2(n-1)} ((n-1) \mu_Z^2 + \sigma_Z^2) \\ 983 \\ 984 = \mathbb{E}[\tilde{R}^2] \left(\frac{2}{n} \mu_Z^2 \right) + (\mathbb{E}[\tilde{R}])^2 \left(\frac{2n-2}{n} \mu_Z^2 + \frac{2}{n} \sigma_Z^2 \right).$$

985 We have:
986

$$987 \text{Var}(\tilde{G}_q) = C_1 + C_2 - C_3 = \mathbb{E}[\tilde{R}^2] \left(\frac{1}{n-1} \sigma_Z^2 \right) + (\mathbb{E}[\tilde{R}])^2 \left(-\frac{1}{n-1} \sigma_Z^2 \right) \\ 988 \\ 989 = \frac{\sigma_Z^2}{n-1} (\mathbb{E}[\tilde{R}])^2 - (\mathbb{E}[\tilde{R}])^2 \\ 990 \\ 991 = \frac{\sigma_Z^2}{n-1} \text{Var}(\tilde{R}).$$

992 For a given prompt, \tilde{R} takes 1 with probability p and -1 with probability $1-p$, leading to its
993 variance of $4p(1-p)$. We obtain the final variance of the per-prompt gradient estimator:
994

$$995 \text{Var}(\tilde{G}_q) = \frac{\sigma_Z^2}{n-1} \cdot 4p(1-p).$$

1000 This completes the proof. □
1001

1002 A.2 PROOFS OF SECTION 5

1003 *Proof of Theorem 5.1.* For clarity and continuity, we restate problem (6) before proceeding with the
1004 proof:
1005

$$1006 \min \quad \sum_{q \in \mathcal{B}_t} a_q \frac{n_q - 1}{n_q^2} \\ 1007 \text{s.t.} \quad \sum_{q \in \mathcal{B}_t} n_q = C \\ 1008 \quad L \leq n_q \leq U \quad \forall q \in \mathcal{B}_t. \tag{10}$$

1009 Let $V(\{n_q\})$ be the objective function of the above problem. We compute the first and second
1010 derivatives of the objective function with respect to each coordinate n_q :
1011

$$1012 \frac{\partial V}{\partial n_q} = -a_q \frac{n_q - 2}{n_q^3}.$$

1013 Since $n_q \geq L \geq 3$, so for all q , $\frac{\partial V}{\partial n_q} < 0$. Thus, V is decreasing with respect to each n_q on the
1014 feasible set.
1015

1016 For the second derivatives:
1017

$$1018 \frac{\partial^2 V}{\partial n_q \partial n_{q'}} = 0 \quad \forall q \neq q', \quad \frac{\partial^2 V}{\partial n_q^2} = a_q \frac{2n_q - 6}{n_q^4} \geq 0 \quad \forall q \quad (\text{Since } n_q \geq L \geq 3, \text{ and } a_q \geq 0)$$

1026 Therefore, V is convex and decreasing in each n_q on the feasible set
 1027

$$1028 \quad 1029 \quad 1030 \quad \left\{ n \in \mathbb{R}^B : \sum_{q \in \mathcal{B}_t} n_q = C, \quad L \leq n_q \leq U \quad \forall q \right\}.$$

1031 Hence, the minimizer exists and is unique whenever the feasible set is nonempty $BL \leq C \leq BU$.
 1032

1033 The Lagrangian function is

$$1034 \quad 1035 \quad 1036 \quad \mathcal{L} = \sum_{q \in \mathcal{B}_t} a_q \frac{n_q - 1}{n_q^2} + \lambda \left(\sum_{q \in \mathcal{B}_t} n_q - C \right) + \sum_{q \in \mathcal{B}_t} \mu_q (L - n_q) + \sum_{q \in \mathcal{B}_t} \nu_q (n_q - U)$$

1037 where $\lambda \in \mathbb{R}$, and $\mu_q, \nu_q \geq 0$ are Lagrangian multipliers. The KKT conditions are:
 1038

$$1039 \quad -a_q \frac{n_q - 2}{n_q^3} + \lambda - \mu_q + \nu_q = 0 \quad \forall q, \\ 1040 \quad \mu_q \geq 0, \quad \nu_q \geq 0 \quad \forall q, \\ 1041 \quad \mu_q (n_q - L) = 0, \quad \nu_q (n_q - U) = 0 \quad \forall q, \\ 1042 \quad L \leq n_q \leq U \quad \forall q, \\ 1043 \quad \sum_{q \in \mathcal{B}_t} n_q = C.$$

1044 We consider three cases of n_q :
 1045

- 1046 • For each q with $L < n_q < U$, the KKT stationarity condition is

$$1047 \quad 1048 \quad 1049 \quad \lambda = a_q \frac{n_q - 2}{n_q^3},$$

1050 where λ is the Lagrange multiplier for the sum constraint. Note that the right-hand side is
 1051 decreasing in n_q .
 1052

1053 For $n_q = L$, the right-hand side is $a_q \frac{L-2}{L^3}$, and for $n_q = U$, it is $a_q \frac{U-2}{U^3}$. Therefore, for each q
 1054 and any $\lambda \in (a_q \frac{U-2}{U^3}, a_q \frac{L-2}{L^3})$, there is at most one solution n_q to $a_q \frac{n_q - 2}{n_q^3} = \lambda$ in the interior
 1055 (L, U) . If $\lambda \geq a_q \frac{L-2}{L^3}$ or $\lambda \leq a_q \frac{U-2}{U^3}$, there is no interior solution, and the optimum for n_q must
 1056 be at a bound.
 1057

- 1058 • If $n_q = L$, then $\mu_q \geq 0$ and $\nu_q = 0$. According to the KKT condition, we obtain:
 1059

$$1060 \quad 1061 \quad 1062 \quad \lambda = a_q \frac{L-2}{L^3} + \mu_q \geq a_q \frac{L-2}{L^3}.$$

- 1063 • If $n_q = U$, then $\mu_q = 0$ and $\nu_q \geq 0$. According to the KKT condition, we obtain:
 1064

$$1065 \quad 1066 \quad 1067 \quad \lambda = a_q \frac{U-2}{U^3} - \nu_q \leq a_q \frac{U-2}{U^3}.$$

1068 For a value of λ , for each coordinate, the KKT solution for n_q is defined as:
 1069

$$1070 \quad 1071 \quad 1072 \quad 1073 \quad n_q^*(\lambda) = \begin{cases} U & \text{if } \lambda \leq a_q \frac{U-2}{U^3}, \\ \text{the unique solution to } \lambda = a_q \frac{n_q - 2}{n_q^3} & \text{if } a_q \frac{U-2}{U^3} < \lambda < a_q \frac{L-2}{L^3}, \\ L & \text{if } \lambda \geq a_q \frac{L-2}{L^3}. \end{cases}$$

1074 The coupling constraint $\sum_{q \in \mathcal{B}_t} n_q = C$ is enforced by selecting λ such that
 1075

$$1076 \quad 1077 \quad 1078 \quad S(\lambda) \triangleq \sum_{q \in \mathcal{B}_t} n_q^*(\lambda) = C.$$

1079 Each $n_q^*(\lambda)$ is non-increasing in λ since $a_q \frac{n_q - 2}{n_q^3}$ is decreasing and the projection preserves monotonicity. Consequently, $S(\lambda)$ is also non-increasing. In particular:

1080 • As $\lambda \rightarrow -\infty$, $n_q^*(\lambda) \rightarrow U$, so $S(-\infty) = BU$.
 1081
 1082 • As $\lambda \rightarrow +\infty$, $n_q^*(\lambda) \rightarrow L$, so $S(+\infty) = BL$.
 1083

1084 Therefore, for any feasible C with $BL \leq C \leq BU$, there exists a unique λ^* such that $S(\lambda^*) = C$.
 1085 Moreover, because S is non-increasing, finding λ^* can be done by bisection. If $C > BU$ or $C <$
 1086 BL , the problem is infeasible. \square

1087
 1088 *Proof of Theorem 5.2.* For clarity and continuity, we restate Problem 8 before proceeding with the
 1089 proof:

1090
$$\begin{aligned} \min \quad & \sum_{q \in \mathcal{B}_t} a_q \frac{1}{n_q} \\ \text{s.t.} \quad & \sum_{q \in \mathcal{B}_t} n_q = C \\ & L \leq n_q \leq U \quad \forall q \in \mathcal{B}_t \end{aligned} \tag{11}$$

1096 Let $V(\{n_q\})$ be the objective function of the above problem. We compute the first and second
 1097 derivatives of the objective function with respect to each coordinate n_q :

1098
$$\frac{\partial V}{\partial n_q} = -a_q \frac{1}{(n_q - 1)^2}$$

1101 Since $n_q \geq L \geq 3$ and $a_q > 0$, we have $\frac{\partial V}{\partial n_q} \leq 0$ for all q . Thus, V is decreasing with respect to
 1102 each n_q on the feasible set.
 1103

1104 For the second derivatives:

1105
$$\frac{\partial^2 V}{\partial n_q \partial n_{q'}} = 0 \quad \forall q \neq q', \quad \frac{\partial^2 V}{\partial n_q^2} = 2a_q \frac{1}{(n_q - 1)^3} > 0 \quad \forall q$$

1108 Therefore, V is convex and decreasing in each n_q on the feasible set

1109
$$\left\{ n \in \mathbb{R}^B : \sum_{q \in \mathcal{B}_t} n_q = C, \quad L \leq n_q \leq U \right\}.$$

1113 Hence, the minimizer exists and is unique whenever the feasible set is nonempty ($BL \leq C \leq BU$).

1114 The Lagrangian function is

1116
$$\mathcal{L} = \sum_{q \in \mathcal{B}_t} a_q \frac{1}{n_q - 1} + \lambda \left(\sum_{q \in \mathcal{B}_t} n_q - C \right) + \sum_{q \in \mathcal{B}_t} \mu_q (L - n_q) + \sum_{q \in \mathcal{B}_t} \nu_q (n_q - U)$$

1119 where $\lambda \in \mathbb{R}$, $\mu_q, \nu_q \geq 0$. The KKT conditions are:

1121
$$-a_q \frac{1}{(n_q - 1)^2} + \lambda - \mu_q + \nu_q = 0 \quad \forall q$$

1122
$$\mu_q \geq 0, \quad \nu_q \geq 0 \quad \forall q$$

1124
$$\mu_q (n_q - L) = 0, \quad \nu_q (n_q - U) = 0 \quad \forall q$$

1125
$$L \leq n_q \leq U \quad \forall q$$

1127
$$\sum_{q \in \mathcal{B}_t} n_q = C.$$

1129 We consider three cases of n_q :

1131 • For each q with $L < n_q < U$, the KKT stationarity condition is

1133
$$\lambda = a_q \frac{1}{(n_q - 1)^2},$$

1134 where λ is the Lagrange multiplier for the sum constraint. Note that the right-hand side is
 1135 decreasing in n_q since $n_q \geq L \geq 3$.
 1136

1137 For $n_q = L$, the right-hand side is $a_q \frac{1}{(L-1)^2}$, and for $n_q = U$, it is $a_q \frac{1}{(U-1)^2}$. Therefore, for each
 1138 q and any $\lambda \in (a_q \frac{1}{(U-1)^2}, a_q \frac{1}{(L-1)^2})$, there is one solution $n_q = \sqrt{\frac{a_q}{\lambda}} + 1$ to $a_q \frac{1}{(n_q-1)^2} = \lambda$
 1139 in the interior (L, U) . If $\lambda \geq a_q \frac{1}{(L-1)^2}$ or $\lambda \leq a_q \frac{1}{(U-1)^2}$, there is no interior solution, and the
 1140 optimum for n_q must be at a bound.
 1141

- 1142 • If $n_q = L$, then $\mu_q \geq 0$ and $\nu_q = 0$. According to the KKT condition, we obtain:
 1143

$$1144 \quad \lambda = a_q \frac{1}{(L-1)^2} + \mu_q \geq a_q \frac{1}{(L-1)^2}.$$

- 1145 • If $n_q = U$, then $\mu_q = 0$ and $\nu_q \geq 0$. According to the KKT condition, we obtain:
 1146

$$1147 \quad \lambda = a_q \frac{1}{(U-1)^2} - \nu_q \leq a_q \frac{1}{(U-1)^2}.$$

1150 For a value of λ , for each coordinate, the KKT solution for n_q is defined as:
 1151

$$1152 \quad n_q^*(\lambda) = \begin{cases} U & \text{if } \lambda \leq a_q \frac{1}{(U-1)^2}, \\ 1153 \quad \sqrt{\frac{a_q}{\lambda}} + 1 & \text{if } a_q \frac{1}{(U-1)^2} < \lambda < a_q \frac{1}{(L-1)^2}, \\ 1154 \quad L & \text{if } \lambda \geq a_q \frac{1}{(L-1)^2}. \end{cases}$$

1155 The coupling constraint $\sum_{q \in \mathcal{B}_t} n_q = C$ is enforced by selecting λ such that
 1156

$$1157 \quad S(\lambda) := \sum_{q \in \mathcal{B}_t} n_q^*(\lambda) = C.$$

1158 Each $n_q^*(\lambda)$ is non-increasing in λ (since $a_q \frac{1}{(n_q-1)^2}$ is decreasing and the projection preserves mono-
 1159 tonicity), so $S(\lambda)$ is also non-increasing. In particular:
 1160

- 1161 • As $\lambda \rightarrow -\infty$, $n_q^*(\lambda) \rightarrow U$, so $S(-\infty) = BU$.
 1162
- 1163 • As $\lambda \rightarrow +\infty$, $n_q^*(\lambda) \rightarrow L$, so $S(+\infty) = BL$.
 1164

1165 Therefore, for any feasible C with $BL \leq C \leq BU$, there exists a unique λ such that $S(\lambda) = C$. If
 1166 $C > BU$ or $C < BL$, the problem is infeasible. \square
 1167

1171 B STATISTICAL TESTS FOR SECOND-ORDER UNCORRELATION

1172 In this section, we provide statistical tests to validate the assumptions in our paper.
 1173

1174 B.1 FIRST-ORDER CORRELATION TEST VIA FISHER'S METHOD

1175 For each question q , consider the two random variables \tilde{R}_q and \tilde{Z}_q , with n independent observations
 1176

$$1177 \quad \{(\tilde{R}_{q,j}, \tilde{Z}_{q,j})\}_{j=1}^n.$$

1178 **Compute per-question Pearson correlation.** The sample Pearson correlation for question q is
 1179

$$1180 \quad \hat{\rho}_q = \frac{\sum_{j=1}^n (\tilde{R}_{q,j} - \bar{\tilde{R}}_q)(\tilde{Z}_{q,j} - \bar{\tilde{Z}}_q)}{\sqrt{\sum_{j=1}^n (\tilde{R}_{q,j} - \bar{\tilde{R}}_q)^2 \sum_{j=1}^n (\tilde{Z}_{q,j} - \bar{\tilde{Z}}_q)^2}},$$

1181 where
 1182

$$1183 \quad \bar{\tilde{R}}_q = \frac{1}{n} \sum_{j=1}^n \tilde{R}_{q,j}, \quad \bar{\tilde{Z}}_q = \frac{1}{n} \sum_{j=1}^n \tilde{Z}_{q,j}.$$

1188 **Compute per-question p -values.** For each question q , we test the null hypothesis
 1189
 1190
$$H_{0,q} : \rho_q = 0.$$

1191 The p -value p_q is obtained directly from the standard Pearson correlation test.
 1192
 1193 **Combine p -values across questions using Fisher's method.** Let Q be the total number of ques-
 1194 tions. Fisher's method combines the per-question p -values $\{p_q\}_{q=1}^Q$ into a single test statistic:
 1195
 1196
$$\chi_{\text{Fisher}}^2 = -2 \sum_{q=1}^Q \ln p_q.$$

1197 Under the global null hypothesis
 1198
 1199
$$H_0 : \rho_q = 0 \quad \forall q,$$

1200 the statistic χ_{Fisher}^2 follows a chi-squared distribution with $2Q$ degrees of freedom:
 1201
 1202
$$\chi_{\text{Fisher}}^2 \sim \chi_{2Q}^2.$$

1203 **Global p -value and decision rule.** The global p -value for testing H_0 across all questions is
 1204
 1205
$$p_{\text{global}} = \Pr(\chi_{2Q}^2 \geq \chi_{\text{Fisher}}^2).$$

1206 Given a significance level α (e.g., $\alpha = 0.05$), we make the following decision:
 1207
 1208

- If $p_{\text{global}} < \alpha$, we reject the global null hypothesis H_0 , which indicates that at least some of the correlations ρ_q are significantly different from zero across the questions.
- If $p_{\text{global}} \geq \alpha$, we fail to reject H_0 , which supports the hypothesis that the correlations ρ_q are zero for all questions at the significance level α .

1209 We conduct the correlation test described above on a benchmark of $Q = 600$ questions, each with
 1210 $n = 16$ independent rollouts. For each question q , we compute the Pearson correlation between
 1211 \tilde{R}_q and \tilde{Z}_q , obtain the corresponding p -value p_q , and aggregate across all questions using Fisher's
 1212 method to compute the global p -value p_{global} .

1213 We evaluate the policy model π_{θ_t} at four checkpoints during training of Qwen2.5-Math-1.5B,
 1214 corresponding to 0.0, 0.5, 1.0 epochs. At each checkpoint, we report the resulting p_{global} values in
 1215 Table 5. Since all global p -values exceed the chosen significance level $\alpha = 0.05$, we do not reject the
 1216 null hypothesis, which supports our assumption that the correlations ρ_q are zero across all questions.
 1217

Epoch	Global p -value	
	$\tilde{Z}_j = \mathbb{1}^\top H(\tilde{o}_j)$	$\tilde{Z}_j = \ H(\tilde{o}_j)\ _2$
0.0	0.3230	0.7322
0.5	0.3050	0.1108
1.0	0.3050	0.2186

1218 Table 5: Global p -values (p_{global}) across training epochs for Qwen2.5-Math-1.5B.
 1219
 1220

1221 B.2 FIRST-ORDER CORRELATION TEST VIA EDGINGTON'S METHOD

1222 For each question q , let $\hat{\rho}_q$ denote the sample Pearson correlation computed from n independent
 1223 rollouts, and let p_q be the corresponding two-sided p -value for testing the null hypothesis
 1224

$$H_{0,q} : \rho_q = 0.$$

1225 To aggregate evidence across all Q questions, we apply Edgington's sum-of- p method.
 1226
 1227

1228 **Sum of p -values.** Each per-question p_q is treated as a realization of a $\text{Uniform}(0, 1)$ variable under
 1229 its null hypothesis. Edgington's statistic is defined by the simple sum
 1230

$$S_{\text{Ed}} = \sum_{q=1}^Q p_q.$$

1242 **Null distribution.** Under the global null hypothesis
 1243

$$1244 \quad H_0 : \rho_q = 0 \quad \forall q,$$

1245 each $p_q \sim \text{Uniform}(0, 1)$, and therefore
 1246

$$1247 \quad S_{\text{Ed}} \sim \text{Irwin-Hall}(Q),$$

1248 with mean and variance
 1249

$$1250 \quad \mathbb{E}[S_{\text{Ed}}] = \frac{Q}{2}, \quad \text{Var}(S_{\text{Ed}}) = \frac{Q}{12}.$$

1251 For large Q , S_{Ed} is well approximated by a normal distribution:
 1252

$$1253 \quad S_{\text{Ed}} \approx \mathcal{N}\left(\frac{Q}{2}, \frac{Q}{12}\right).$$

1256 **Global p -value and decision rule.** Small values of S_{Ed} indicate joint evidence against H_0 . The
 1257 corresponding one-sided global p -value is

$$1258 \quad p_{\text{global}} = \Phi\left(\frac{S_{\text{Ed}} - Q/2}{\sqrt{Q/12}}\right),$$

1261 where Φ denotes the standard normal CDF. Given a significance level $\alpha = 0.5$, we reject H_0 when
 1262 $p_{\text{global}} < \alpha$.
 1263

1264 We set up the experiment identically to the Fisher’s method test in Appendix B.1, using the same
 1265 benchmark of $Q = 600$ questions, each with $n = 16$ independent rollouts. For each checkpoint of
 1266 the policy model π_{θ_t} , we compute the Edgington statistic and report the global p -value. Since all
 1267 global p -values exceed the chosen significance level $\alpha = 0.05$, we do not reject the null hypothesis,
 1268 which supports our assumption that the correlations ρ_q are zero across all questions.
 1269

Epoch	Global p -value	
	$\tilde{Z}_j = \mathbb{1}^\top H(\tilde{o}_j)$	$\tilde{Z}_j = \ H(\tilde{o}_j)\ _2$
0.0	0.9125	0.7894
0.5	0.8963	0.3964
1.0	0.8912	0.2148

1276 Table 6: Global p -values (p_{global}) across training epochs for Qwen2.5-Math-1.5B using Edging-
 1277 ton’s method.
 1278

1280 B.3 EQUAL VARIANCE TEST VIA LEVENE’S TEST 1281

1282 In the numerical experiments, we have assumed that the variance for \tilde{Z}_q is constant across different
 1283 prompts q . We proceed with a hypothesis test:
 1284

$$1285 \quad H_0 : \sigma_{Z_q}^2 = \sigma_{Z_{q'}}^2, \quad \forall q \neq q', \quad H_1 : \text{At least one } \sigma_{Z_q}^2 \neq \sigma_{Z_{q'}}^2.$$

1287 For each question q , consider the random variable \tilde{Z}_q with n_q independent observations $\{\tilde{Z}_{q,j}\}_{j=1}^{n_q}$.
 1288

1289 **Transform observations for Levene’s test.** Let $Y_{q,j}$ denote the absolute deviation from the per-
 1290 question median:
 1291

$$1291 \quad Y_{q,j} = |\tilde{Z}_{q,j} - \text{median}(\tilde{Z}_{q,1}, \dots, \tilde{Z}_{q,n_q})|.$$

1292 **Compute group means of transformed observations.** The mean of the transformed observations
 1293 for question q is
 1294

$$1295 \quad \bar{Y}_q = \frac{1}{n_q} \sum_{j=1}^{n_q} Y_{q,j},$$

1296 and the overall mean across all questions is
 1297

$$1298 \quad \bar{Y} = \frac{1}{N} \sum_{q=1}^Q \sum_{j=1}^{n_q} Y_{q,j}, \quad N = \sum_{q=1}^Q n_q.$$

$$1299$$

$$1300$$

1301 **Compute Levene's test statistic.** The test statistic is given by
 1302

$$1303 \quad W = \frac{(N - Q) \sum_{q=1}^Q n_q (\bar{Y}_q - \bar{Y})^2}{(Q - 1) \sum_{q=1}^Q \sum_{j=1}^{n_q} (Y_{q,j} - \bar{Y}_q)^2}.$$

$$1304$$

$$1305$$

1306 Under the null hypothesis that the variances are equal across questions,
 1307

$$1308 \quad H_0 : \sigma_{Z_q}^2 = \sigma_{Z_{q'}}^2, \quad \forall q \neq q',$$

$$1309$$

1310 the statistic W approximately follows an F -distribution with $Q - 1$ and $N - Q$ degrees of freedom
 1311 $W \sim F_{Q-1, N-Q}$.

1312 **Compute p -value and decision rule.** The p -value for testing H_0 is
 1313

$$1314 \quad p_{\text{Levene}} = \Pr(F_{Q-1, N-Q} \geq W).$$

$$1315$$

1316 Given a significance level α (e.g., $\alpha = 0.05$), we make the following decision:
 1317

- 1317 • If $p_{\text{Levene}} < \alpha$, we reject H_0 , indicating that the variances of \tilde{Z}_q differ across questions.
- 1318 • If $p_{\text{Levene}} \geq \alpha$, we fail to reject H_0 , the hypothesis that the variances are equal across all ques-
 1319 tions, at the significance level α .

1320 We conduct the variance homogeneity test described above on a benchmark of $Q = 600$ questions,
 1321 each with $n = 16$ independent rollouts. We perform Levene's test across all questions to assess
 1322 the equality of variances. We evaluate the policy model π_{θ_t} at four checkpoints during training of
 1323 Qwen2.5-Math-1.5B, corresponding to 0.0, 0.5, 1.0 epochs. At each checkpoint, we report the
 1324 resulting global p -values p_{Levene} in Table 7. Since all p_{Levene} exceed the chosen significance level
 1325 $\alpha = 0.05$, we can not reject the null hypothesis, which supports our assumption that the variances
 1326 $\sigma_{Z_q}^2$ are equal across all questions.
 1327

1328 Epoch	1329 Global p -value	
	1330 $\tilde{Z}_j = \mathbb{1}^\top H(\tilde{o}_j)$	1330 $\tilde{Z}_j = \ H(\tilde{o}_j)\ _2$
1331 0.0	0.5019	0.2705
1332 0.5	0.4132	0.4785
1333 1.0	0.3847	0.3847

1334 Table 7: p_{Levene} from Levene's test across training epochs for Qwen2.5-Math-1.5B, assessing
 1335 variance homogeneity of \tilde{Z}_q .
 1336

1338 **B.4 EQUAL VARIANCE TEST VIA O'BRIEN'S TEST**

1340 In the numerical experiments, we have assumed that the variance for \tilde{Z}_q is constant across different
 1341 prompts q . We proceed with a hypothesis test:
 1342

$$1343 \quad H_0 : \sigma_{Z_q}^2 = \sigma_{Z_{q'}}^2, \quad \forall q \neq q', \quad H_1 : \text{At least one } \sigma_{Z_q}^2 \neq \sigma_{Z_{q'}}^2.$$

$$1344$$

1345 For each question q , consider the random variable \tilde{Z}_q with n_q independent observations $\{\tilde{Z}_{q,j}\}_{j=1}^{n_q}$.
 1346

1347 **Transform observations for O'Brien's test.** Let $Y_{q,j}$ denote O'Brien's transformation of the ob-
 1348 servations:
 1349

$$Y_{q,j} = \frac{(n_q - 1.5)n_q(\tilde{Z}_{q,j} - \bar{\tilde{Z}}_q)^2 - 0.5s_q^2(n_q - 1)}{(n_q - 1)(n_q - 2)},$$

1350 where \tilde{Z}_q is the sample mean for question q , and s_q^2 is the unbiased sample variance for question q .
 1351

1352 **Compute group means of transformed observations.** The mean of the transformed observations
 1353 for question q is

$$1354 \quad \bar{Y}_q = \frac{1}{n_q} \sum_{j=1}^{n_q} Y_{q,j},$$

1357 and the overall mean across all questions is

$$1358 \quad \bar{Y} = \frac{1}{N} \sum_{q=1}^Q \sum_{j=1}^{n_q} Y_{q,j}, \quad N = \sum_{q=1}^Q n_q.$$

1362 **Compute O'Brien's test statistic.** The test statistic is given by
 1363

$$1364 \quad W_{\text{OB}} = \frac{(N - Q) \sum_{q=1}^Q n_q (\bar{Y}_q - \bar{Y})^2}{(Q - 1) \sum_{q=1}^Q \sum_{j=1}^{n_q} (Y_{q,j} - \bar{Y}_q)^2}.$$

1367 Under the null hypothesis that the variances are equal across questions,
 1368

$$1369 \quad H_0 : \sigma_{Z_q}^2 = \sigma_{Z_{q'}}^2, \quad \forall q \neq q',$$

1371 the statistic W_{OB} approximately follows an F -distribution with $Q - 1$ and $N - Q$ degrees of freedom
 1372 $W_{\text{OB}} \sim F_{Q-1, N-Q}$.

1373 **Compute p -value and decision rule.** The p -value for testing H_0 is
 1374

$$1375 \quad p_{\text{OB}} = \Pr(F_{Q-1, N-Q} \geq W_{\text{OB}}).$$

1376 Given a significance level α (e.g., $\alpha = 0.05$), we make the following decision:
 1377

- 1378 • If $p_{\text{OB}} < \alpha$, we reject H_0 , indicating that the variances of \tilde{Z}_q differ across questions.
 1379
- 1380 • If $p_{\text{OB}} \geq \alpha$, we fail to reject H_0 , the hypothesis that the variances are equal across all questions,
 1381 at the significance level α .

1382 We conduct the variance homogeneity test described above on a benchmark of $Q = 600$ questions,
 1383 each with $n = 16$ independent rollouts. We perform O'Brien's test across all questions to assess
 1384 the equality of variances. We evaluate the policy model π_{θ_t} at three checkpoints during training
 1385 of Qwen2.5-Math-1.5B, corresponding to 0.0, 0.5, 1.0 epochs. At each checkpoint, we report
 1386 the resulting global p -values p_{OB} in Table 8. Since all p_{OB} exceed the chosen significance level
 1387 $\alpha = 0.05$, we cannot reject the null hypothesis, which supports our assumption that the variances
 1388 $\sigma_{Z_q}^2$ are equal across all questions.
 1389

1390 Epoch	1391 Global p -value	
	$\tilde{Z}_j = \mathbb{1}^\top H(\tilde{o}_j)$	$\tilde{Z}_j = \ H(\tilde{o}_j)\ _2$
1393 0.0	0.1612	0.3009
1394 0.5	0.1215	0.2563
1395 1.0	0.1229	0.2420

1396 Table 8: p_{OB} from O'Brien's test across training epochs for Qwen2.5-Math-1.5B, assessing
 1397 variance homogeneity of \tilde{Z}_q .
 1398

1400 **C ADDITIONAL INFORMATION ON NUMERICAL EXPERIMENTS**
 1401

1402 **Hyperparameters.** We curate a list of important training hyperparameters for our experiment in
 1403 Table 9.

Table 9: Hyperparameter configuration.

Category	Hyperparameter	Value / Setting
Optimizer	Optimizer	AdamW
	Learning rate	1×10^{-6}
	Warm-up	20 rollout steps
rollout	Prompt batch size	512
	Responses per prompt	6/8/Dynamic
Training	Mini-batch size	512
	Max generation length	10 240 tokens
	Temperature	1.0

C.1 ADDITIONAL INFORMATION ON ABLATION STUDIES

Inverse-accuracy allocation. We allocate more rollout budget to prompts with lower empirical accuracy. Concretely, letting acc_i denote the running accuracy estimate for prompt i , we set target weights $w_i \propto (1 - \text{acc}_i + \epsilon)$ and normalize to meet the global budget and per-prompt bounds.

Inverse-variance allocation. We allocate more rollout budget to prompts whose answers exhibit lower variance. Letting σ_i^2 be the (running) answer variance estimate, we set $w_i \propto 1/(\sigma_i^2 + \epsilon)$ with the same normalization.

Both heuristics are implemented via a continuously relaxed, constrained optimization that enforces the total-budget and box constraints; we solve it with an online solver and then map fractional solutions to integers using the rounding heuristic.

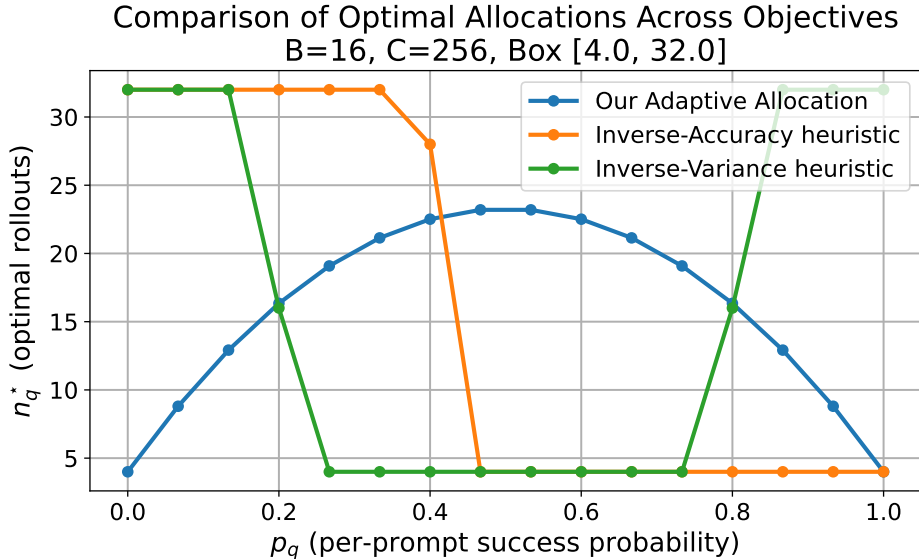


Figure 3: Comparison of optimal rollout allocations produced by different heuristics versus our proposed variance-aware allocation strategy. The figure plots the optimal number of rollouts n_i^* against prompt difficulty p_i , highlighting how our method allocates budget differently from inverse-accuracy and inverse-variance baselines.

C.2 PROMPT TEMPLATE.

During training, we only use one prompt template for every prompt in the dataset. There are two prompt templates, one for mathematical reasoning and one for tool-augmented reasoning.

1458
1459
1460
1461

Figure 4: Prompt template for mathematical reasoning

Solve the following math problem step by step. The last line of your response should be of the form `Answer: $Answer` (without quotes) where `$Answer` is the answer to the problem. Do not wrap `$Answer` with `\boxed{}`.

current question: {{question}}

Below are two examples for format reference.

Example question 1: Solve for x : $3x - 5 = 16$.

Response:

Add 5 to both sides: $3x = 21$.

Divide both sides by 3: $x = 7$.

Answer: 7

Solve the current question. Remember to put your answer on its own line after "Answer:".

1477
1478
1479
1480
1481

Figure 5: Prompt template for tool augmented reasoning

In this environment you have access to a set of tools you can use to assist with the user query.

You may perform multiple rounds of function calls.

In each round, you can call one or more functions.

Here are available functions in JSONSchema format:
\n```json\n{func_schemas}\n```

In your response, you need to first think about the reasoning process in the mind and then conduct function calling to get the information or perform the actions if needed. \
The reasoning process and function calling are enclosed within <think> </think> and <tool_call> </tool_call> tags. \
The results of the function calls will be given back to you after execution, \
and you can continue to call functions until you get the final answer for the user's question. \
Finally, if you have got the answer, enclose it within \\boxed{{}} with latex format and do not continue to call functions, \
i.e., <think> Based on the response from the function call, I get the weather information. </think> The weather in Beijing on 2025-04-01 is \\[\\boxed{{20C}} \\].

For each function call, return a json object with function name and arguments within <tool_call></tool_call> XML tags:
<tool_call>
{ "name": <function-name>, "arguments": <args-json-object> }
</tool_call>

1510

1511

1512

D ALGORITHMS

1513

1514

1515

1516

1517

The algorithm capturing the complete flow the posterior update for the Gaussian Process is provided in Algorithm 1.

1518

Algorithm 1 Recursive GP Posterior Update

1519

1520

1521

1522

1523

1524

1525

1526

1527

1528

1529

1530

1531

1532

1533

1534

1535

1536

1537

1538

1539

1540

Require: Mini-batch \mathcal{B}_t ; rollout allocation $\{n_q\}_{q=1}^{\mathcal{B}_t}$; prior mean $m_t(\mathcal{D}) \in \mathbb{R}^Q$, kernel matrix $\Sigma \in \mathbb{R}^{Q \times Q}$;

- 1: **for** each $q \in \mathcal{B}_t$ **do**
- 2: # Run n_q rollouts and observe outcomes $\tilde{R}_j \in \{-1, 1\}$
- 3: $\bar{R}_q \leftarrow \frac{1}{n_q} \sum_{j=1}^{n_q} \tilde{R}_j$
- 4: $\hat{g}_q \leftarrow \text{sigmoid}^{-1} \left(\text{clip} \left(\frac{\bar{R}_q + 1}{2}, \epsilon, 1 - \epsilon \right) \right)$
- 5: **end for**
- 6: $g_t^{\text{observe}} \leftarrow (\hat{g}_q)_{q \in \mathcal{B}_t}$
- 7: Partition m_t and Σ according to \mathcal{B}_t and \mathcal{B}_t^c
- 8: $m_{t, \mathcal{B}_t^c}^* \leftarrow m_{t, \mathcal{B}_t^c} + \Sigma_{\mathcal{B}_t^c \mathcal{B}_t} \Sigma_{\mathcal{B}_t \mathcal{B}_t}^{-1} (g_t^{\text{observe}} - m_{t, \mathcal{B}_t})$
- 9: $\Sigma^* \leftarrow \Sigma_{\mathcal{B}_t^c \mathcal{B}_t^c} - \Sigma_{\mathcal{B}_t^c \mathcal{B}_t} \Sigma_{\mathcal{B}_t \mathcal{B}_t}^{-1} \Sigma_{\mathcal{B}_t \mathcal{B}_t^c}$
- 10: **for** $q = 1$ **to** Q **do**
- 11: **if** $q \in \mathcal{B}_t$ **then** $m_{t+1}(x_q) \leftarrow \hat{g}_q$ **else** $m_{t+1}(x_q) \leftarrow m_{t, \mathcal{B}_t^c}^*(x_q)$ **end if**
- 12: **end for**
- 13: $\hat{p}_{t+1} = \text{sigmoid}(m_{t+1}(\mathcal{D}))$
- 14: **return** $\{\hat{p}_{t+1}\}, m_{t+1}$

1541

1542

1543

1544

1545

1546

1547

1548

1549

1550

1551

1552

1553

1554

1555

1556

1557

Algorithm 2 Heuristic rounding for integer rollout allocation

1558

1559

1560

1561

1562

1563

1564

1565

1566

1567

1568

1569

1570

1571

1572

1573

1574

1575

1576

1577

1578

1579

1580

1581

1582

1583

1584

1585

E EXTENSION TO CONTINUOUS REWARDS

1586

1587

1588

1589

1590

1591

1592

1593

1594

1595

1596

1597

1598

1599

This section details the necessary adaptations to our predictive rollout allocation strategy for the case where the reward $R(\tilde{o}_j)$ is a real-valued random variable. All definitions, assumptions, and notation follow the main text unless otherwise stated.

1590

1591

1592

1593

1594

1595

1596

1597

E.1 GRADIENT VARIANCE FOR CONTINUOUS REWARDS

1598

1599

1600

1601

1602

1603

1604

1605

We first state the analogues of our variance propositions for the continuous reward setting. The proofs are intermediate results from proofs for binary case in Appendix A.

1566
 1567 **Proposition E.1** (Dr. GRPO gradient variance, continuous reward). *Let $R(\tilde{o}_j) = \tilde{R}$ be a real-
 1568 valued random variable with variance $\text{Var}(\tilde{R})$. If Assumption 4.1 holds and $\text{Var}(\tilde{Z}) = \sigma_Z^2$, then the
 1569 variance of the per-prompt projected Dr. GRPO gradient estimator with n rollouts is*

$$1570 \text{Var}(\tilde{G}) = \frac{(n-1)\sigma_Z^2}{n^2} \text{Var}(\tilde{R}).$$

1572
 1573 **Proposition E.2** (RLOO gradient variance, continuous reward). *Let $R(\tilde{o}_j) = \tilde{R}$ be a real-valued
 1574 random variable with variance $\text{Var}(\tilde{R})$. If Assumption 4.1 holds and $\text{Var}(\tilde{Z}) = \sigma_Z^2$, then the
 1575 variance of the per-prompt projected RLOO gradient estimator with n rollouts is*

$$1576 \text{Var}(\tilde{G}) = \frac{\sigma_Z^2}{n-1} \text{Var}(\tilde{R}).$$

1579 E.2 GAUSSIAN PROCESS PREDICTION OF REWARD VARIANCE

1581 For continuous rewards, the per-prompt gradient variance depends on $\text{Var}(\tilde{R}_q)$, which is not directly
 1582 observable prior to rollout. To predict this quantity, we replace the GP model for success probability
 1583 with a GP model for reward variance. Specifically, for each prompt q , we model the reward variance
 1584 as $v_{q,t} = \text{softplus}(g_t(x_q)) = \log(1 + \exp(g_t(x_q)))$, where g_t is a latent GP as in the main text.
 1585 After observing rewards $\{\tilde{R}_{q,j}\}_{j=1}^{n_q}$, we compute the sample variance \tilde{s}_q^2 and set the observation for
 1586 the latent variable as $\hat{g}_{q,t} = \log(\exp(\tilde{s}_q^2) - 1)$. The GP posterior update and recursive prediction
 1587 steps proceed identically, replacing the sigmoid link with the softplus link.

1589 E.3 BUDGET ALLOCATION OPTIMIZATION

1590 Given predicted reward variances $\widehat{\text{Var}}(\tilde{R}_q)$, we define $a_q := \sigma_{Z_q}^2 \widehat{\text{Var}}(\tilde{R}_q)$. The continuous relax-
 1591 ation of the rollout allocation problem for Dr. GRPO becomes
 1592

$$1593 \min \left\{ \sum_{q \in \mathcal{B}_t} a_q \frac{n_q - 1}{n_q^2} : \sum_{q \in \mathcal{B}_t} n_q = C, L \leq n_q \leq U, n_q \in \mathbb{R} \forall q \right\},$$

1596 and for RLOO,

$$1597 \min \left\{ \sum_{q \in \mathcal{B}_t} a_q \frac{1}{n_q - 1} : \sum_{q \in \mathcal{B}_t} n_q = C, L \leq n_q \leq U, n_q \in \mathbb{R} \forall q \right\}.$$

1600 The optimal solutions are given by Theorems 5.1 and 5.2 in the main text, now with the updated
 1601 definition of a_q . The rounding procedure described in Appendix D applies without modification.

1603 F TRAINING EVOLUTION COMPARISON

1605 In this section, we assess the robustness and stability of our method by retraining
 1606 Qwen2.5-Math-1.5B using GRPO, RLOO, and their VIP-augmented counterparts (GRPO+VIP,
 1607 RLOO+VIP) across **five random seeds**. Figures 6 and 7 report the mean and standard deviation for
 1608 multiple performance metrics (*best@32*, *maj@32*, *mean@32*).

1609 To ensure that all training trajectories are directly comparable, **every model is trained on the same**
 1610 **dataset under identical optimization settings**: the same fixed ordering of 17k training prompts,
 1611 one epoch of training, a batch size of 512, mini-batch size of 64, and rollout budget per batch of 512
 1612 * 8. As a result, each gradient step corresponds to the same amount of data and computation across
 1613 all methods.

1614 Across all seeds and evaluation checkpoints, we observe consistent and pronounced improvements
 1615 from using VIP:

1617 **(i) Faster early-stage learning.** VIP yields substantial gains in the early phase of training. For
 1618 example, on AIME2024 *mean@32*, RLOO+VIP reaches an accuracy of **0.0316** by step 10, whereas
 1619 RLOO reaches only **0.0056**—a **6× increase**. Similar trends appear in both *best@32* and *maj@32*
 metrics across AIME2024 and AIME2025.

1620
1621 **(ii) Steeper and more reliable improvement per gradient step.** VIP consistently increases the
1622 slope of the learning curve. Its trajectories rise smoothly and monotonically, while the baselines
1623 (particularly GRPO on AIME2025 *best@32*) often progress slowly or temporarily plateau between
1624 steps 10–20. This shows that variance-aware allocation accelerates the effective learning rate with-
1625 out introducing instability.

1626 **(iii) Increased training stability.** VIP reduces variance across seeds and produces smoother learn-
1627 ing curves, reflecting more stable gradient updates. This aligns with the goal of variance-informed
1628 allocation: reducing gradient noise directly translates into more predictable and reliable optimization
1629 dynamics.

1630 Together, these results demonstrate that VIP improves both the **speed** and the **stability** of GRPO
1631 and RLOO training, leading to faster convergence and consistently higher performance throughout
1632 the entire training trajectory.

1633

1634

1635

1636

1637

1638

1639

1640

1641

1642

1643

1644

1645

1646

1647

1648

1649

1650

1651

1652

1653

1654

1655

1656

1657

1658

1659

1660

1661

1662

1663

1664

1665

1666

1667

1668

1669

1670

1671

1672

1673

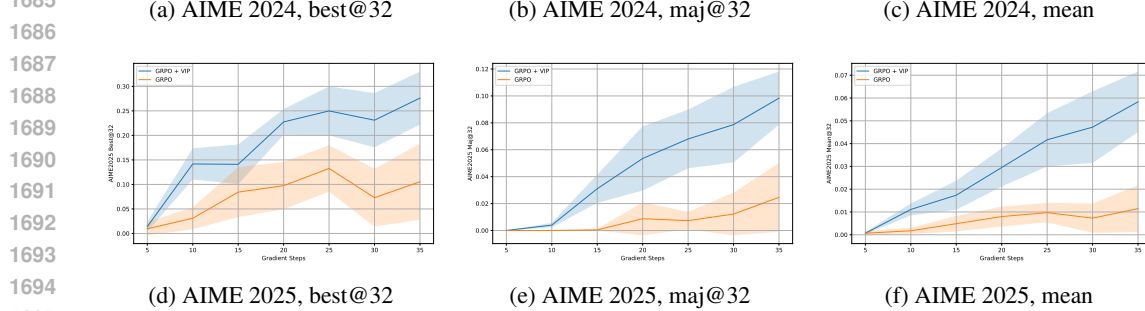
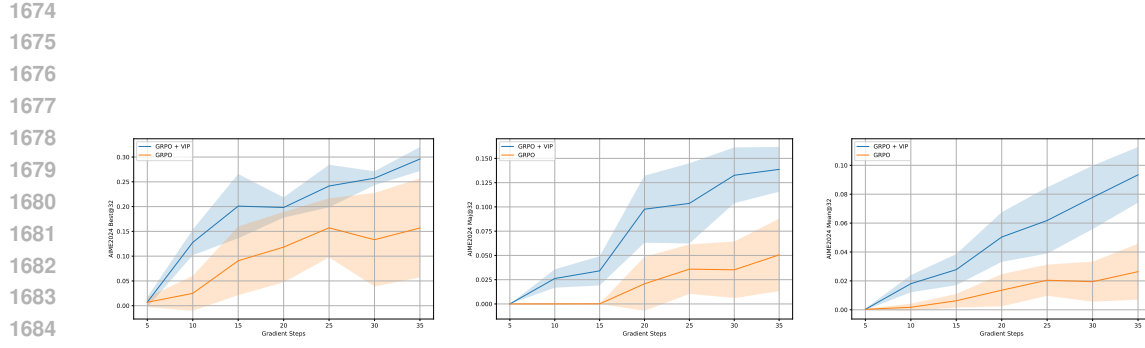


Figure 6: GRPO vs. GRPO+VIP on AIME 2024 and 2025 across different accuracy metrics.

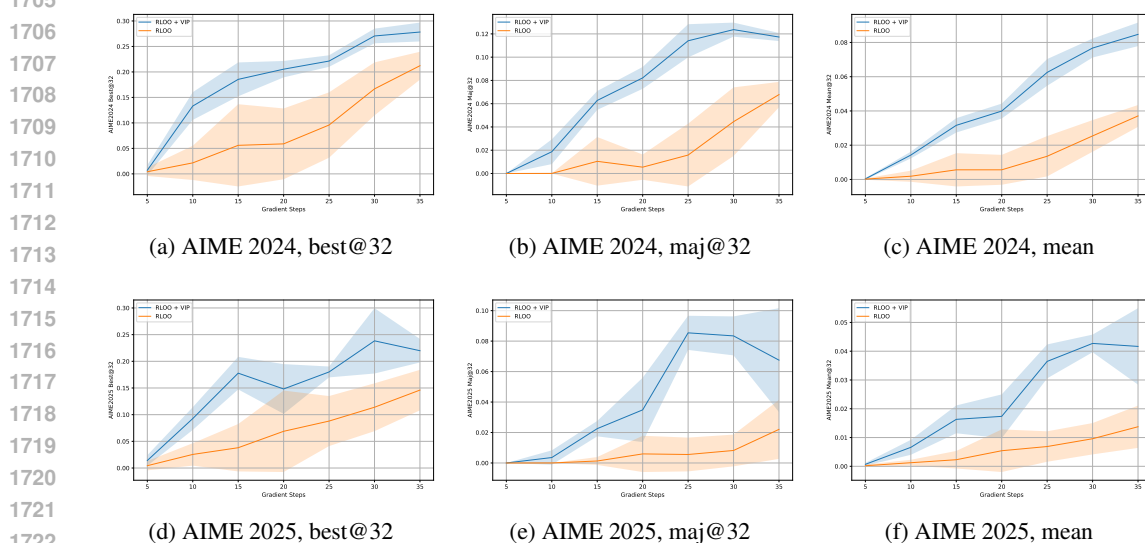


Figure 7: RLOO vs. RLOO+VIP on AIME 2024 and 2025 across different accuracy metrics.